Proposal for dielectron measurements in heavy-ion collisions at J-PARC with E16 upgrades

K. Aoki[1,2], T. Chujo[3], G. David[4], H. Ekawa[5], S. Esumi[3], P. Garg[4], T. Gunji (*Spokesperson*)[6], T. Hachiya[5,7], H. Hamagaki[8,6], H. Harada[9], B.S. Hong[10], Y. Ichikawa[11], M. Inaba[12], J. Kamiya[9], M. Kaneta[13], E.J. Kim[14], M. Kinsho[9], M. Kitazawa[15,16], Y. Kondo[9], Y. Kwon[18], Y. Miake[3,11], H. Miyatake[2,11], Y. Morino[1,2], K. Moriya[9], S. Nagamiya[5,2,11], M. Nakagawa[5], T. Nakamura[2], Y. Nara[17], M. Naruki[19,11], T. Niida[3], K. Nishio[11], T. Nonaka[3], K. Oyama[8], K. Ozawa (*Spokesperson*)[1,2,3], P.K. Saha[9], T.R. Saito[5,20,21], T. Sakaguchi[22], H. Sako (*Spokesperson*)[11,3], K. Shigaki[23], S. Shimansky[24], M. Shimomura[7], H. Takahashi[1,2], F. Tamura[9], H. Tamura[13,11], J. Tamura[9], K.H. Tanaka[1,2], and S. Yokkaichi[5]

[1]J-PARC Center, High Energy Accelerator Research Organization, Tokai, Ibaraki 319-1195, Japan
[2]KEK, High Energy Accelerator Research Organization, Tsukuba, Ibaraki 305-0801, Japan
[3]Tomonaga Center for the History of the Universe, University of Tsukuba, Tsukuba, Ibaraki 305-8571, Japan
[4]Department of Physics and Astronomy, Stony Brook University, SUNY, Stony Brook, New York 11794-3800, USA
[5]RIKEN, Wako, Saitama 351-0198, Japan
[6]Center for Nuclear Study, the University of Tokyo, Wako, Saitama 351-0198, Japan
[7]Department of Mathematical and Physical Science, Nara Woman's University, Nara, Nara 630-8506, Japan
[8]Department of Engineering, Nagasaki Institute of Applied Science, Nagasaki, Nagasaki 851-0193, Japan
[9]J-PARC Center, Japan Atomic Energy Agency, Tokai, Ibaraki 319-1195, Japan

[10]Department of Physics, Korea University, Seongbuk-gu, Seoul 136-701, Republic of Korea
[11]Advanced Science Research Center, Japan Atomic Energy Agency, Tokai, Ibaraki 319-1195, Japan
[12]Division of Industrial Technology, Tsukuba University of Technology, Tsukuba, Ibaraki 305-8520, Japan
[13]Graduate School of Science, Tohoku University, Sendai, Miyagi 980-8578, Japan
[14]Department of Physics, College of National Science, Chonbuk National University, Jeonju-si, Jeollabuk-do 54896, Republic of Korea
[15]Department of Physics, School of Science, Osaka University, Toyonaka, Osaka 560-0043, Japan
[16]J-PARC Branch, KEK Theory Center, High Energy Accelerator Research Organization, Tokai, Ibaraki 319-1106, Japan
[17]Faculty of International Liberal Arts, Akita International University, Yuwa, Akita 010-1292, Japan
[18]Department of Physics, Yonsei University, Seoul, 03722, Republic of Korea
[19]Department of Physics, Kyoto University, Kyoto 606-8502, Japan
[20]GSI Helmholtzzentrum für Schwerionenforschung GmbH, 64291 Darmstadt, Germany
[21]Johannes Gutenberg University of Mainz, 55122 Mainz, Germany
[22]Physics Department, Brookhaven National Laboratory, Upton, NY 11973-5000, USA
[23]Graduate School of Science, Hiroshima University, Higashi-Hiroshima, Hiroshima 739-8526, Japan
[24]Joint Institute for Nuclear Research, 141980 Dubna, Moscow Region, Russia

June 14, 2021

Executive Summary

We propose the first heavy-ion collision experiment at J-PARC using the J-PARC E16 spectrometer with moderate detector and DAQ upgrades. This experiment makes use of the high-intensity heavy-ion beams with 2-12 AGeV to be provided by the newly-designed heavy-ion acceleration scheme that uses the 3-GeV RCS and MR at J-PARC. This experiment will play a precursory role in future heavy-ion experiments at J-PARC.

The heavy-ion collisions at this energy region will serve as a unique opportunity to explore a very high density medium possibly existing in the universe, such as inside the neutron stars. Theoretical models predict the existence of first phase transition, critical point, and various new phases such as color-superconductivity at the density region, though these have not been confirmed experimentally. The goal of the new experiment is to search for the phase transition to a new state of matter composed of deconfined quarks and gluons at extremely high baryon densities using a di-electron probe. A di-electron measurement provides the emission rates of the virtual photons from the hot medium directly without suffering from the final interaction, which sheds light on the initial temperature and space-time evolution of the medium.

Among various information accessible through the di-electron spectra, in this proposal, we especially focus on the two phenomena that will be explored for the first time at $\sqrt{s_{NN}}$ = 3 - 5 GeV. First, through the measurement of a di-electron spectrum at intermediate mass region ($1 \lesssim M_{ee} \lesssim 3$ GeV/c^2) we will investigate the thermal radiation of the virtual photons from the partonic phase and the hadronic phase. Since the thermal radiation is directly connected to temperature and density of the medium. this measurement will provide us with very critical information on the creation of the partonic medium in heavy-ion collisions at J-PARC energy.

Second, the spectrum at the low invariant-mass region will also be analyzed in detail for exploring the medium modification of vector mesons in the hot and dense medium. The measurement of such phenomena in the cold nuclear matter is now ongoing at the E16 experiment. The extension of this experiment to heavy-ion collisions will enrich the physics of the E16 experiment.

The proposed experiment will measure mass spectra of electron-positron pairs in Au+Au collisions. For the experiment, accelerations of Au ions and transportation of the beam to the Hadron Experimental Facility are required. The acceleration of heavy-ions will be implemented by adding a new injector and a new booster. The heavy-ion beam from the new booster will be injected into the existing RCS and MR and can be accelerated up to the beam energy of 12 AGeV. We have two plans for the injector and the booster, such as the final design and the fast approach for the current proposed experiment. For the proposed experiment, we will construct a new heavy-ion LINAC and reuse the KEK 500-MeV booster proton synchrotron (KEK-BS). The length of the HI LINAC is half of the originally designed one.

The experiment will be performed with the upgraded E16 spectrometer. The designed intensity of the 12 AGeV heavy-ion beam is 10^8 per spill, which corresponds to the same beam power of the 30 GeV proton beam intensity of 10^{10}/spill that is currently used for E16. The radiation level with this heavy-ion beam intensity is evaluated, and the experiment is possible without modifications of the radiation shielding

and beam dumps. To cope with higher hit multiplicities in the heavy-ion collisions, the E16 spectrometer needs to be upgraded especially in the forward region. The E16 spectrometer consists of 26 modules and each module has a Silicon Strip Detector, three layers of GEM Trackers, Hadron Blind Detector, and Lead-Glass calorimeter. The forward 4 modules, which are surrounded by the beam pipe, need to be modified to preserve the tracking and electron identification performances. In the forward modules, innermost GEM Tracker and outermost Lead-Glass calorimeter will be replaced with a Silicon Strip Detector and a fine-segmented crystal $PbWO_4$ calorimeter, respectively. The current data acquisition system is optimized for p-A collisions and the maximum trigger rate is limited by 1 kHz. The data acquisition system has to be upgraded accordingly in order to inspect as many minimum bias Au+Au collisions as possible. We have two approaches under consideration for the upgrade of the data acquisition system, where one is to enhance the trigger capability from 1 kHz to 30 kHz by optimizing the APV readouts and upgrading the FPGA readout firmware with online processing and feature extraction supported to reduce the data throughput and then processing and writing data in parallel into disk. The other approach is to introduce the triggerless and free steaming data acquisition system, which has been under development in ALICE and LHCb experiment at the LHC. By replacing the front-end with the one which supports the continuous readout, data from detectors is continuously read out. By utilizing hardware acceleration such as FPGA and GPU, data is further processed, event building and data reconstruction are executed online and compressed data is written in disk.

We request 100 days of the beam time with a Au beam at the intensity of 1.0×10^8 ions per spill and the energy of 12 AGeV for the first measurement to determine the medium temperature with an accuracy of about 10%.

This experiment will be a pioneering experiment for future heavy-ion physics at J-PARC energy. The series of the experiments will be followed aiming at searching for the critical phenomena associated with the 1st or 2nd order of phase transition, characterizing the properties of quark matter and deconfinment and chiral transitions, and searching for the new state of matter such as quarkyonic matter or a color superconductor.

1 Physics Motivation

Medium described by Quantum Chromodynamics (QCD) is a highly non-trivial condensed matter system having various phase transitions. It is known that hadronic medium undergoes the phase transition to the quark-gluon plasma (QGP) in extremely dense and/or hot environment as schematically shown in Figure. 1. This phase transition occurs with the chiral restoration, which is the phase transition of the vacuum. Even inside the hadronic phase, the medium modification of hadrons, such as the mass shift, is expected to occur due to the modification of the vacuum structure in the medium. These phenomena are tightly connected with the fundamental properties of QCD, such as the spontaneous chiral symmetry breaking and confinement of quarks. Therefore, their investigation is quite important and useful in revealing these non-perturbative aspects of QCD.

The experimental search for the dense and hot medium interacting via the strong interaction has been made actively over last few decades both from experimental and theoretical researches. Experimentally, the relativistic heavy-ion collisions are unique tools for creating and investigating the hot and dense media on the Earth. Active experimental analyses for studying properties of QGP are ongoing all over the world at RHIC, LHC, and GSI. At RHIC started in 2000, creation of the QGP has been established through the measurement of various observables, such as the collective flow of hadrons and the medium modification of the jets. The experiments at RHIC have also revealed non-trivial properties of QGP, such as the small viscosity/entropy ratio that indicates the strong-coupling nature of the QGP near the critical temperature. In 2009, the heavy-ion collisions at yet higher collision energies began at the LHC, at which more detailed study of the QGP has been being carried out. The heavy-ion collisions also serve as unique experiments for producing exotic hadrons and hyper nuclei, measuring the interaction between them [1, 2, 3] (please update references; MK). These measurements are another important purpose of the heavy-ion collisions.

An interesting feature of the phase transition to QGP is that the order of the transition is changed with the variation of the density of the medium. Though it is known from lattice QCD numerical simulations that the phase transition is a crossover at zero baryon density, many theoretical models predict that the order of the phase transition turns to the first order at high baryon density [4]. As a result, at least one end point of the first-order transition line must exist in the QCD phase diagram as shown in Fig. 1. Furthermore, in dense and cold quark matter new exotic phases called color superconducting states are expected to realize triggered by the condensation of di-quarks. Experimental search for these phase transitions is one of the most intriguing but ambitious subjects of the heavy-ion collisions after the finding of the QGP.

In relativistic heavy-ion collisions, the temperature and baryon density of the medium created by the collisions can be varied by changing the collision energy. At the highest collision energy of RHIC, $\sqrt{s_{NN}} = 200$ GeV, the baryon density of the hot medium produced by the collisions is vanishingly small because baryons in the colliding nuclei penetrate with each other and pass through the collision point due to large initial momentum. For yet larger $\sqrt{s_{NN}}$, baryon density becomes much smaller although temperature T becomes larger with increasing $\sqrt{s_{NN}}$. On the other hand, by

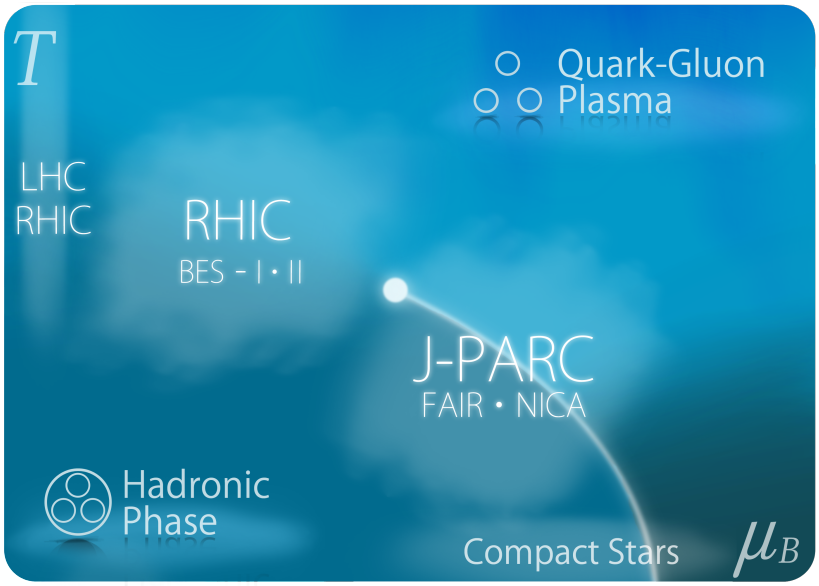

Figure 1: Phase diagram of QCD.

lowering $\sqrt{s_{NN}}$ from the top-RHIC energy the baryon density becomes larger because baryons in the colliding nuclei tend to stop inside the hot medium at the collision point. From the simulations of dynamical models [5], the baryon density is expected to enhance down to $\sqrt{s_{NN}} \simeq 5$ GeV; for the collisions with much smaller $\sqrt{s_{NN}}$ the baryon density becomes lower because the collision energy is not sufficient to compress the medium. The highest baryon density realized at $\sqrt{s_{NN}} \simeq 5$ GeV is expected to exceed more than five times normal nuclear density [5]. This density is comparable with the densest medium in the Universe that realizes at the core of the neutron stars. The heavy-ion collisions enable us to probe the medium under such an extreme condition and to obtain information on the properties of neutron stars by the experiments on the Earth.

The search for the phase structure of QCD at high baryon density using this $\sqrt{s_{NN}}$ dependence of the heavy-ion collisions is one of the hottest topics of the heavy-ion collisions after 2010. At RHIC, the so-called beam-energy scan program that performs heavy-ion collisions for $\sqrt{s_{NN}} = 3 \sim 40$ GeV has been done from 2010 to 2021 for this purpose. The experiments for $\sqrt{s_{NN}} = 3 \sim 10$ GeV are also ongoing at GSI and SPS. As will be discussed in Sec. 1.4, new heavy-ion facilities aiming at the same goal are under construction in GSI and JINR. The search for the QCD critical point and the first-order phase transition is the most important subject among them. These experiments performed in various facilities all over the world with various collision energies will play complementary roles to explore the phase structure of QCD.

In this proposal, we propose a first heavy-ion collision experiment using accelerators in J-PARC and the spectrometers of the J-PARC E16 experiment with the upgrades of the detectors, readout, and data acquisition systems. The heavy-ion beams will be provided by the newly developed heavy-ion injector, and after the acceleration by the

3-GeV RCS and MR in J-PARC up to $E_{\rm lab} \simeq 12$ GeV ($\sqrt{s_{_{NN}}} = 4.9$ GeV) at maximum, supplied to hadron hall. The heavy-ion beams will promote the J-PARC to an experimental facility to explore the hot and dense medium and will open up rich experimental subjects. As discussed in Appendix, we plan to realize the heavy-ion collisions with highest rate in the world by supplying the heavy-ion beams with the world highest intensity. These experiments will play the leading role in exploring the dense medium among experiments performed all over the world. In the first heavy-ion suggested proposed in this proposal, as a pilot experiment prior to this main experiment we generate the heavy-ion beams with lower intensity and perform the experiments focusing on the measurements of di-electron spectra as a function of di-electron invariant mass and pair p_T for various collision centralities and discuss the phase transition to the thermally excited partonic medium at high baryon densities and the in-medium modifications of the hadron spectral functions. Since the maximum collision energy of these experiments, $\sqrt{s_{_{NN}}} = 4.9$ GeV, is suitable for creating the densest medium in heavy-ion collisions, the heavy-ion collision experiments in J-PARC will serve as a unique opportunity to explore the medium inside the neutron stars.

Among various observables in heavy-ion collisions, the di-lepton (di-electron and di-muon) production spectra are unique observables that provide us with direct information on the medium property. The di-leptons are produced by the decay of virtual photons. Through this observable one thus can measure the emission spectrum of virtual photons from the dense medium. The outstanding property of the di-leptons is that the di-leptons and virtual photons do not interact with the medium by the strong interaction. Therefore, the production rate from the medium is directly observed without contamination of the final interaction.

The spectrum of the di-lepton production as a function of invariant mass, m_{ll}, provides us with various information on the hot medium depending on the region of m_{ll}. At the low-mass region ($m_{ll} \lesssim 1$ GeV), the production rate is dominated by the decays of hadrons. This m_{ll} region thus is suitable for studying the medium modification of vector mesons that are important for characterizing the dynamics of the hadronic phase of the medium. In fact, non-trivial di-lepton spectra that cannot be explained by vacuum hadrons have been observed in the low-mass region at SPS. The medium modification of ϕ meson in the cold nuclear matter has also been observed at the KEK-PS E325 experiment, and the succeeding experiment is now ongoing at the E16 experiment. At intermediate-mass region ($1 \lesssim m_{ll} \lesssim 3$ GeV) the main contribution for the di-lepton production is the thermal radiation from the partonic and hadronic phase. This m_{ll} region is suitable for studying the basic thermal properties, such as temperature, of the medium.

The strong penetration of di-leptons through medium would also allow us to explore the color-superconducting phases, the phases of QCD in extremely dense and cold matter characterized by the di-quark condensations. In one of the color-superconducting states called the color-flavor locked phase, a gluon and a photon mix together and consequently gluons can decay into di-lepton pairs [6]. Such decays will produce a peak in the di-lepton spectrum at the gluon mass. It has also been suggested that an anomalous enhancement of the di-lepton production occurs at low m_{ll} near but above the critical temperature of the color superconductivity due to pair-annihilations of the

di-quark soft modes developed near the phase boundary [7]. These signals will serve as a first opportunity to access the color-superconducting phases.

In the following, we discuss physical phenomena that are probed by the di-lepton measurements in more detail by classifying them into thermal di-leptons (Sec. 1.1), in-medium modifications of vector mesons (Sec. 1.2), and search for color superconductivity (Sec. 1.3).

1.1 Thermal Di-lepton

One of the main purposes of this proposed experiment is to discover the (first-order) phase transition of the chiral and deconfinement transition at high baryon density. One of the experimental clearest evidence for the first-phase transition is an observation of a plateau structure in the "caloric curve", which is the dependence of the temperature on the excitation energy of the system. Also in nuclear matter, the first-order liquid-gas phase transition has been widely believed to exist. The smoking gun of the liquid-gas phase transition was the plateau structure in the caloric curve as shown in Figure 2[8]. Therefore, it is important to measure the temperature of the high density matter as a function of the collision energy or centrality, which are the proxy of the excitation energy, and to search for the (first-order phase) deconfinement transition.

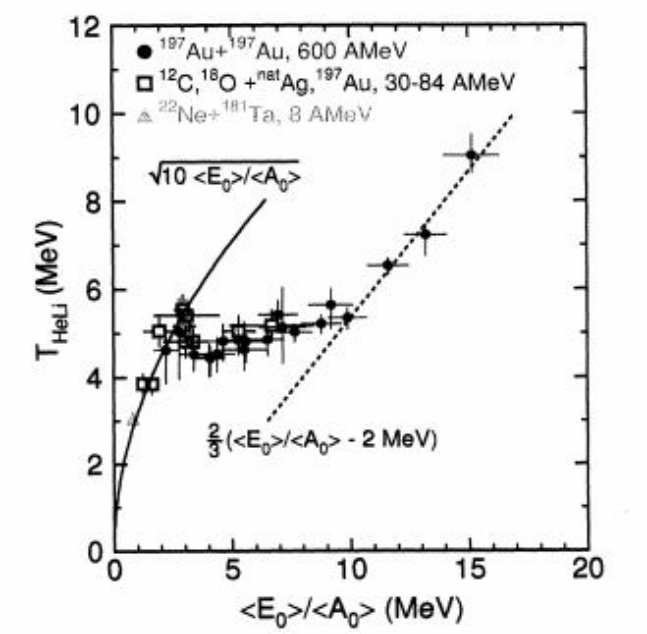

Figure 2: Caloric curve of nuclei determined by the dependence of the isotope temperature. This Figure is taken from Ref. [8].

The high density matter created with relativistic heavy-ion collisions has space-time evolution and the temperature of the matter changes dynamically during the evolution of the system. In order to observe the plateau-like structure, a measurement of the temperature at the hottest stage shortly after the collisions is neces-

sary. Under such circumstances, measurements of di-lepton pairs with higher invariant masses ($m_{e^+e^-} \geq 0.5 - 1$ GeV/c^2) provide an excellent probe for the information near the hottest stage since di-leptons are penetrating in the matter without any strong interactions with medium constituents and thermal di-leptons created by annihilation or collisions between thermal quarks, anti-quarks, and gluons contribute only at high temperature regions like heavy quarks at RHIC and LHC [9]. Therefore, the temperature extracted from the thermal di-lepton pairs with high masses is very sensitive to the early hot stages. "High mass" enough to extract the information in the early stage depends on the collision energy. For example, the thermal di-lepton pairs with $M_{l^+l^-} > 0.4$ GeV/c^2 can extract the information in the early stage at the SIS18 energy ($\sqrt{s_{NN}} \sim 2.4$ GeV/c^2), corresponding to $M_{l^+l^-} > 1.2$ GeV/c^2 at the SPS energy ($\sqrt{s_{NN}} \sim 17$ GeV/c^2)[10].

The temperature of the matter can be extracted from the invariant mass spectrum of the thermal di-lepton pairs using the relation that the yield (dN_{ee}/dM_{ee}) is approximately proportional to $(MT)^{3/2}\exp(-M/T)$ in the case of $M \gg T$. This extraction method has the advantage of being unaffected by a collective expansion of the matter, whereas the pair p_T distribution is suffered from the blue shift due to a radial expansion of the system. The NA60 experiment observed di-muon excess above $M_{\mu\mu} \geq 1$ GeV/c^2 in In+In collisions at CERN-SPS [11, 12]. The upper panel in Fig. 3 shows an excess spectrum of di-muon invariant mass and a comparison with several model calculations. The bottom plot shows T_{eff} as a function of mass, where T_{eff} is obtained for each mass range assuming that $dN/dm_T \propto \exp(-m_T/T_{eff})$. Below 1 GeV/$c$, T_{eff} increases since this region is dominated by di-muons from the hadronic phase and the radial expansion of the system leads to the blue shift of the pair p_T spectrum. On the contrary, above 1 GeV/c, T_{eff} decreases since di-muons from the partonic phase are dominated and the radial expansion is not fully developed at this early stage.

Figure 4 shows the temperature of the density matter extracted from the di-lepton invariant mass spectrum measured by NA60 [13] and HADES [14] as a function of the collision energy [15, 16]. In Fig. 4, the purple line and the magenta dashed line show the initial temperature ($T_{initial}$) obtained from a fireball model and the temperature extracted from the di-lepton invariant mass spectrum above 1 GeV/c^2 (T_{slope}) calculated from a coarse-graining transport approach, respectively [17, 10]. The critical temperature of the phase transition with $\mu_B = 0$ calculated by recent lattice QCD calculation is also indicated in the green dashed area in Fig. 4[18]. In the case of heavy-ion collisions with several $\sqrt{s_{NN}}$ GeV, the critical temperature becomes even lower because of large μ_B. At higher energy, due to the longer space-time evolution enough hot to create di-lepton pairs with $M_{l^+l^-} > 1$ GeV/c^2 T_{slope} is affected by the whole the partonic evolution and gets smaller than $T_{initial}$. This difference becomes smaller at lower energy due to the shorter lifetime where di-lepton pairs with $M_{l^+l^-} > 1$ GeV/c^2 can be created. At J-PARC energy, it is expected that T_{slope} can well approximate $T_{initial}$ meaning that the di-electron measurements can probe the matter at the initial temperature and the maximum density.

Another strong point of di-electron measurements at J-PARC is correlated di-electron decays from heavy quarks are negligible at $M_{l^+l^-} > 1$ GeV/c^2 and, therefore, this mass range is best suited for searching for the thermal di-electron pairs, while

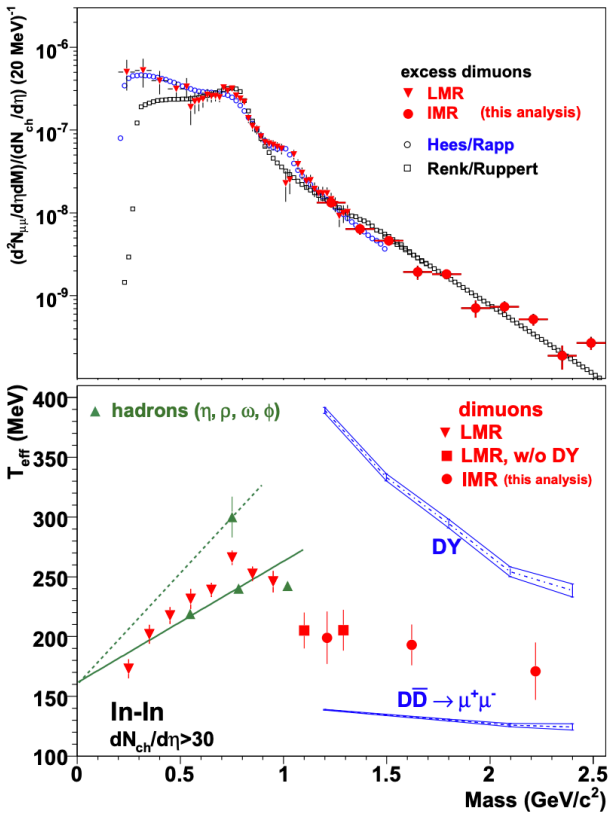

Figure 3: Upper: Acceptance-corrected mass spectra of the excess dimuons in NA60 collaboration [11, 12]. Bottom: The inverse slope parameter T_{eff} of the excess m_T spectra vs. di-muon mass.

correlated pairs from heavy quarks significantly contribute at higher energies.

The caloric curves of $T_{initial}$ and T_{slope} in Fig. 4 do not include any effects of the first-order deconfinement phase transition. If the first-order phase transition exists, the T_{slope} curve will be modified and a plateau-like structure is expected to emerge, unlike Fig. 4. Since the energy range of the J-PARC is expected to be the region where the phase transition exists according to the recent lattice calculation [18], a measurement of the matter temperature via the thermal di-electron spectrum with high invariant masses at J-PARC energy is an ideal tool to discover the first-order phase transition and to have a firm conclusion that a new state of matter, which differs from the ordinal hadronic matters, is formed.

1.2 Mass Modification of Low-mass Vector Mesons

One of the most important properties to characterize QCD phases is the restoration of the chiral symmetry, since the phase transition occurs with the chiral restoration. To study the chiral symmetry in a finite temperature and/or density matter, measurements of hadron properties, such as mass and decay width, in the matter are essentially

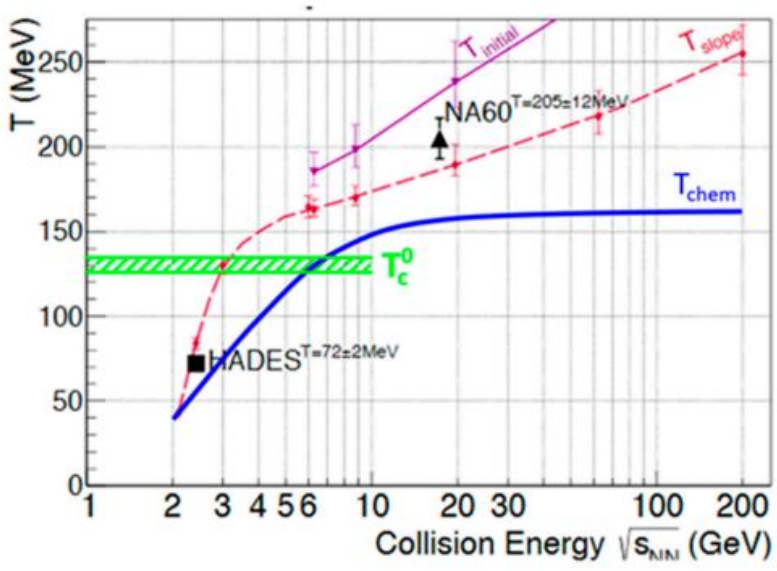

Figure 4: The temperature of the dense matter extracted from di-lepton spectra measured by NA60[13] and HADES[14] as a function of the collision energy. The purple line and the magenta dashed line show the initial temperature ($T_{initial}$) and the temperature extracted from the di-lepton spectra from model calculations [17, 10]. This figure is taken from Refs. [15, 16].

important. Because such hadron properties are tightly connected with the spontaneous chiral symmetry breaking and confinement of quarks.

In this context, measurements of hadron properties in the hot and/or dense matter attract wide interests in the field of hadron physics. Especially, mass spectra of vector mesons, such as ρ, ω and ϕ mesons, were measured in several experiments, since the mass spectra of the vector mesons can be connected with the amount of $\langle \bar{q}q \rangle$ condensate, which is an order parameter of the chiral symmetry restoration, in the matter [19]. Mass spectra are measured using the lepton decays of the vector mesons to avoid the final state interactions of the decayed particles with the matter. Thus, di-lepton measurements are also important for the measurements.

Among those measurements, NA60 at CERN has one of the most successful results[20]. Figure 5 shows invariant mass spectra of $\mu^+\mu^-$ pairs measured by the NA60 experiment. The result shows significant modifications of ρ meson mass spectra.

The HADES experiment also measured di-electron spectra as we discussed in the previous section [14]. Results of the HADES experiments show a significant excess of yields compared to the known hadronic sources in vacuum as shown at Figure 6. It should be understood as a sum of modified ρ meson mass contributions and thermal radiation.

The mass distribution below $\sim$ 0.9 GeV/c^2 after the subtraction of the known hadronic sources in vacuum is believed to be dominated by the medium ρ contribution. Then, the mass distribution in this region is suitable for investigating the medium effect of ρ. Indeed, the clear bumps structure due to ρ is clearly visible in the NA60

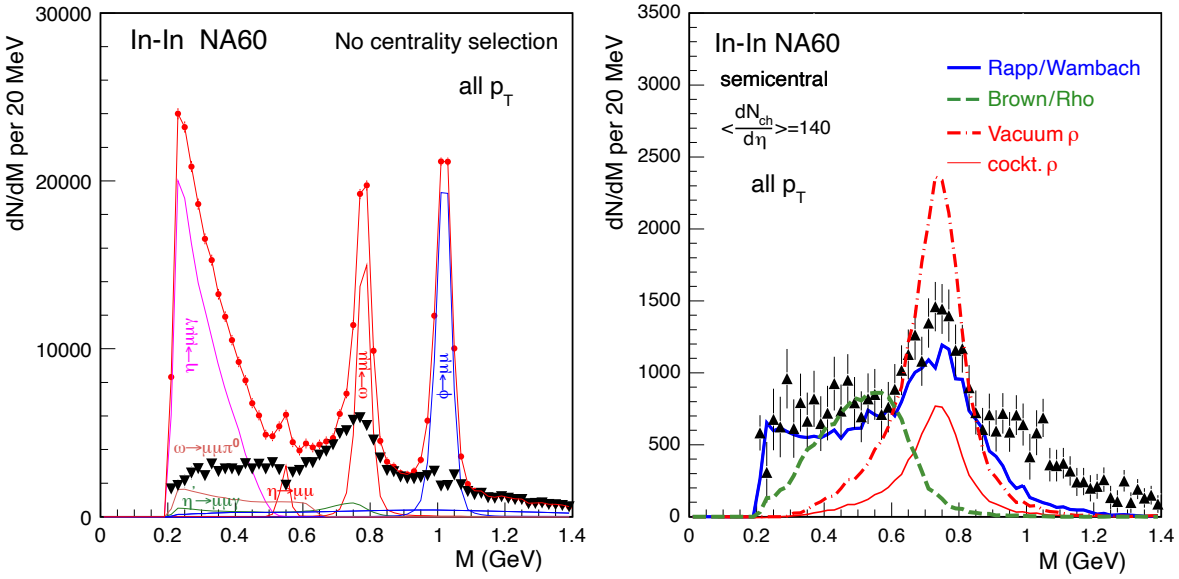

Figure 5: Invariant mass spectra of $\mu^+\mu^-$ pairs measured by the NA60 experiment. Red dots show a spectrum after combinatorial background subtraction and contributions of known hadronic sources are represented as lines (Left). Black triangles show the remaining ρ meson contributions (Left, Right). Theoretical calculations are shown in dotted lines (Right). This figure is taken from Ref. [20].

result, but not in the HADES. It seems that this is because the temperature, density, or degree of freedom of the medium changes depending on the difference in collision energy between the NA60 and the HADES. It is interesting to study how it changes between the two, but currently, no measurement is accurate enough to discuss the mass shape in this region. Therefore, it is of great significance to measure it at J-PARC.

We mention that the di-electrons in this region have another crucial role. Since the di-electrons with low invariant mass are created at almost every stage of the interacting high density matter (namely, fireball), the total excess yield of the low-mass di-electron (total yield after subtraction hadronic sources in vacuum) serves as a "chronometer" of the fireball. Theoretical calculation of a coarse-grained UrQMD transport shows a strong correlation between the total excess yield with $0.3 < M_{e^+e^-} < 0.7$ GeV/c^2 and the fireball lifetime [17]. Therefore, the measurement of these di-electrons can determine the lifetime of the fireball directly.

If the high density matter undergoes the first-order phase transition, the system will pass through the mixed phase. The lifetime of the fireball becomes longer due to the latent heat of the matter than in the case of a smooth cross-over from hadronic to partonic phase. It increases the total excess yield of the di-electrons with $0.3 < M_{e^+e^-} < 0.7$ GeV/c^2 substantially and results in its non-monotonous collision energy dependence [21]. The characteristics of the phase transition can be clarified from the measurement of the di-electrons in this region.

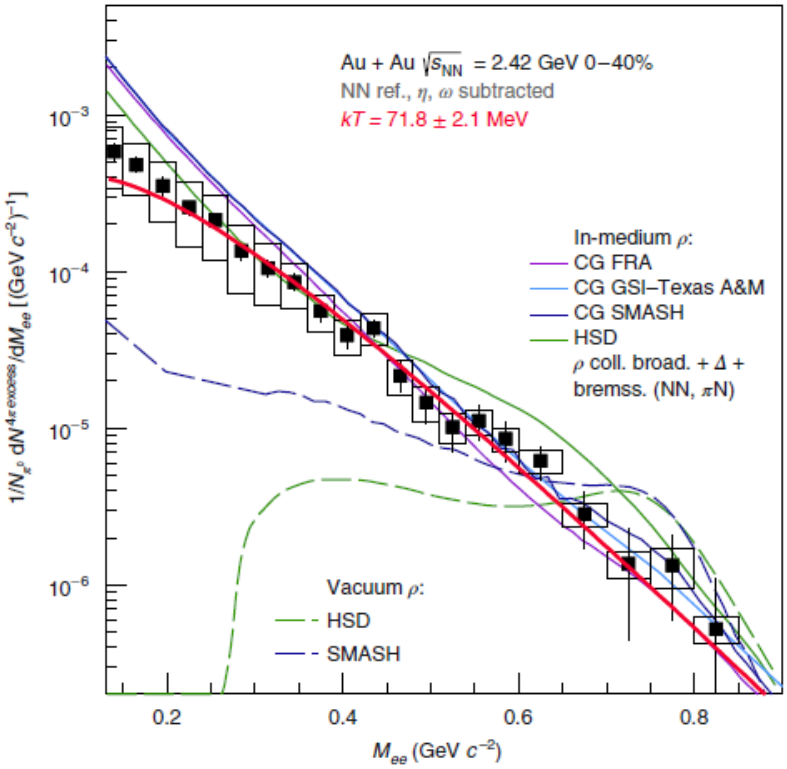

Figure 6: Invariant mass spectra of e^+e^- pairs measured by the HADES experiment. η and ω contributions are subtracted and the acceptance is corrected. This figure is taken from Ref. [14].

1.3 Color Superconductivity

The di-electron spectra measured at the J-PARC energy would enable us to study the color superconducting phases. The measurement of color superconductivity (CSC) in heavy-ion collisions is a challenging task because of two reasons. First, as the CSC is expected to be realized in cold quark matter, say $T \lesssim 50$ MeV, the creation of such cold medium would be difficult in heavy-ion collisions. Second, the chance to realize the CSC is, even if it were possible, limited to the primordial stage in heavy-ion collisions. Therefore, even if the CSC is created by the collisions, the signal generated inside the phase will be blurred by the final interaction during the evolution after the transition to the normal quark matter. Because of these reasons, the measurement of CSC is usually considered to be difficult.

However, the use of the di-leptons will resolve the second problem, since the di-leptons scarcely interact with the medium once they are produced. The signal produced at the primordial stage thus can reach the experimental detectors directly without contamination by the interaction with the medium. The di-lepton emission from the color-flavor locked (CFL) phase, which is the CSC state realized in the high density limit, has been calculated in Ref. [22]. A characteristic enhancement at low m_{ll} inside

the CFL phase has been predicted, which would be used for the signal of the onset of this state. In the CFL phase, a gluon and a photon mix together. As a consequence, gluons can decay into di-lepton pairs [6]. Such decays will produce a peak in the di-lepton spectrum at the gluon mass, which is nonzero inside the CFL phase.

Another possibility to probe the CSC is to use the precursory phenomena of this phase [23]. Near the critical temperature of CSC, the strong di-quark correlations are developed as the soft mode of the CSC. The effect of these di-quark correlations on the di-lepton production has been calculated in Ref. [7], and it has been shown that the pair-annihilation of di-quarks produces an anomalous enhancement of di-leptons at small m_{ll}. The advantage for using this behavior as the signal is that such di-quark modes can be developed even well above the critical temperature. Therefore, such a signal would be observed even if the CSC itself were not created by the collisions. This provides a solution for the first problem raised at the beginning of this subsection.

The detailed analyses of the di-electron spectra at J-PARC, at which the highest baryon density can be created, will enable to probe the onset of the ultimate form of matter in extremely dense environment for the first time.

1.4 Competing Experiments

As discussed already, the heavy-ion collisions aiming at the analysis of dense and hot QCD medium are one of the hottest topics in hadron physics and actively carried out all over the world. At RHIC, the second phase of the beam-energy scan program (RHIC-BES-II) that performs the heavy-ion collisions in a wide range of the collision energy, $3.0 < \sqrt{s_{NN}} < 20$ GeV has just finished and data analysis are ongoing [24]. The NA61/SHINE in SPS experiment has been also performed varying size of the colliding system with similar but slightly lower energy range ($3 \lesssim \sqrt{s_{NN}} \lesssim 17$ GeV) [25]. The experiments with yet lower energies are ongoing at the HADES in GSI ($\sqrt{s_{NN}} \sim 2.4$ GeV) [26]. There are future experimental plans to perform the heavy-ion collisions at the MPD experiment in JINR and the CBM experiment in GSI [27, 28]. These situations are summarized in Figure 7. As this figure shows, exploring the phase diagram of QCD by the beam-energy scan is a hot topic that receives strong attention all over the world.

The collision energy and the interaction rate that will be realized by the first stage of the heavy-ion collisions is shown by the rectangle in Fig. 7. As the figure shows, the beam intensity of the J-PARC even at the first stage is stronger than any existing experiment in this energy region, and after the completion of a full spectrometer and HI injector, a new J-PARC heavy-ion experiment (J-PARC-HI) will achieve the highest interaction rate even including the planned experiment.

The heavy-ion collisions with various collision energies play complementary roles in exploring the phase diagram of QCD (See, Fig. 1). Among these experiments, this proposal will play a unique role in exploring the di-electron spectrum at $\sqrt{s_{NN}} \sim 5.1$ GeV, since the di-lepton spectra in this energy region have not been measured in the previous experiments. The first measurement in this energy region is an exciting topic that will provide us with valuable information on the densest medium in the Universe.

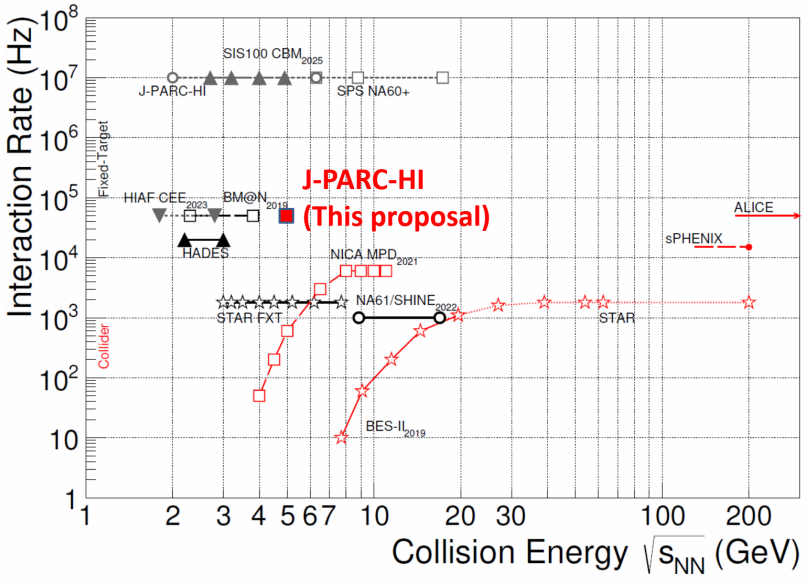

Figure 7: Summary of $\sqrt{s_{NN}}$ and beam intensity of the heavy-ion experiments aiming at the search for dense medium [29].

After finishing the experiments in this proposal, we plan to upgrade the heavy-ion injector and spectrometers to realize the heavy-ion beams with the highest intensity in the world and detailed analyses of various observables as described in Appendix A. This future experiment with 10^7 interaction rate will pioneer the experimental study of the dense medium among the complementary experiments by its strong intensity.

2 Experimental Apparatus

The proposed experiment will measures mass spectra of electron-positron pairs in Au+Au collisions. Accelerations of Au ions and transportation of the beam to the Hadron Experimental Facility is required. The acceleration of heavy-ions will be implemented by adding a new injector and a new booster ring. The heavy-ion beam from the new booster ring will be injected into the existing RCS and MR and can be accelerated up to the beam energy of 12 AGeV. We have two plans for the injector and the booster, such as the final design and the fast approach for the current proposed experiment. For the proposed experiment, we will construct a new heavy-ion LINAC and reuse KEK 500-MeV booster proton synchrotron (KEK-BS). The HI linac has a half size of the final design.

The experiment will be performed with the upgraded E16 spectrometer. To cope with higher hit multiplicities in the heavy-ion collisions, the E16 spectrometer needs to be upgraded especially in the forward region. The E16 spectrometer consists of 26 modules and each module has a Silicon Strip Detector (SSD), three layers of GEM Trackers (GTR), Hadron Blind Detector (HBD), and Lead-Glass calorimeter (LG). The forward 4 modules, which is surrounded the beam pipe, needs to be modified to preserve the tracking and electron identification performances. In the forward modules, innermost GEM Tracker and outermost Lead-Glass calorimeter will be replaced with a Silicon Strip Detector and a fine-segmented crystal $PbWO_4$ calorimeter, respectively. Current data acquisition system is optimized for p+A collisions and the maximum trigger rate is limited by 1 kHz. The data acquisition system has to be upgraded accordingly in order to inspect as many minimum bias Au+Au collisions as possible.

We will start measurements in Au+Au collision and have data acquisition in lighter systems, such as carbon, calcium, later. Also, we are planning to have hadron measurements in future.

2.1 Heavy-ion Beams

We have proposed a high-intensity heavy-ion (HI) driver in combination with a new HI injector and the existing J-PARC accelerators, which are the 3-GeV RCS and MR as a high-intensity proton driver [30]. As described in the proposal paper, the driver aims to accelerate a high-intensity HI beams up to uranium (U) to the energy of 11 GeV/nucleon (AGeV). Ions lighter than uranium can be accelerated up to 11-15 AGeV. The new HI injector is composed of a new HI LINAC and a HI booster ring, whose design parameters of the high-intensity acceleration scheme for U ion beam in J-PARC HI are listed in Table 1.

For the proposed experiment, we are proposing a new version of the acceleration scheme with lower costs (we call it "low-intensity scheme"). The HI injector is composed of a new HI LINAC and the KEK 500-MeV booster proton synchrotron (KEK-BS). The HI LINAC is with the half length of the originally designed one. On the other hand, we reuse the KEK-BS [31] as the booster ring, which was used as the injector to the 12-GeV Proton Synchrotron (KEK-12GeV-PS) at KEK and has a quarter size of the originally designed booster ("the high-intensity HI booster"). The KEK-BS is

composed of eight combined function magnets, which have the dipole field for deflection and the quadrupole field for focusing. Hence, there is no flexible optics at the ring, and the number of injection particles is lower than the high-intensity booster by the factor 10^{-3}. The ion species required by the experiment range from light ions to gold (Au). In the low-intensity scheme for Au, the space charge effect is at a negligible level because the beam intensity is lower than that of proton beam accelerated at present by the order of 10^{-3}. For the lower-intensity scheme, the designed maximum energy and the intensity of heavy-ions up to Au delivered from the MR to experimental beam line are 12-15 AGeV and 1.0×10^{8}, respectively. The various ion species are required such as deuteron, Carbon, Oxygen, Calcium and Au. Design parameters of Au are shown in Table 2.

Table 1: Design parameters of the high-intensity acceleration scheme for the U beam.

Accelerator	Extraction energy	Intensity (particle/pulse)
New HI LINAC	20 AMeV	2.0×10^{11}
New HI booster	67 AMeV	1.5×10^{11}
RCS	735 AMeV	1.1×10^{11}
MR	11.06 AGeV	4.0×10^{11}
$\sqrt{s_{NN}}$ (U+U)	4.9 GeV	

Table 2: Design parameters of the low-intensity acceleration scheme for the Au beam in this proposal.

Accelerator	Extraction energy	Intensity (particle/pulse)
New HI LINAC	9.3 AMeV	1.0×10^{9}
KEK-BS	32.1 AMeV	2.0×10^{8}
RCS	500 AMeV	4.0×10^{7}
MR	11.5 AGeV	1.0×10^{8}
$\sqrt{s_{NN}}$ (Au+Au)	5.0 GeV	

2.2 Hadron Experimental Facility and High-momentum Beam Line

The proposed experiment will be performed at the high-momentum beam line in J-PARC Hadron Experimental facility. The beam transport is basically the same as in the J-PARC E16 experiment except for the beam branching point to the high-momentum beam line. There are two options for the beam transport to the high-momentum beam line: A Lambertson septum magnet and beam swinger magnets depending on the phase of the Hadron Experimental Facility. Figure 8 shows a conceptual view of the two options at the beam branching point in the case of the heavy-ion beam. The upper panels shows the Lambertson magnet option. The position of the Lambertson magnet is modified in the vertical direction and the Lambertson magnet is used as a kicker

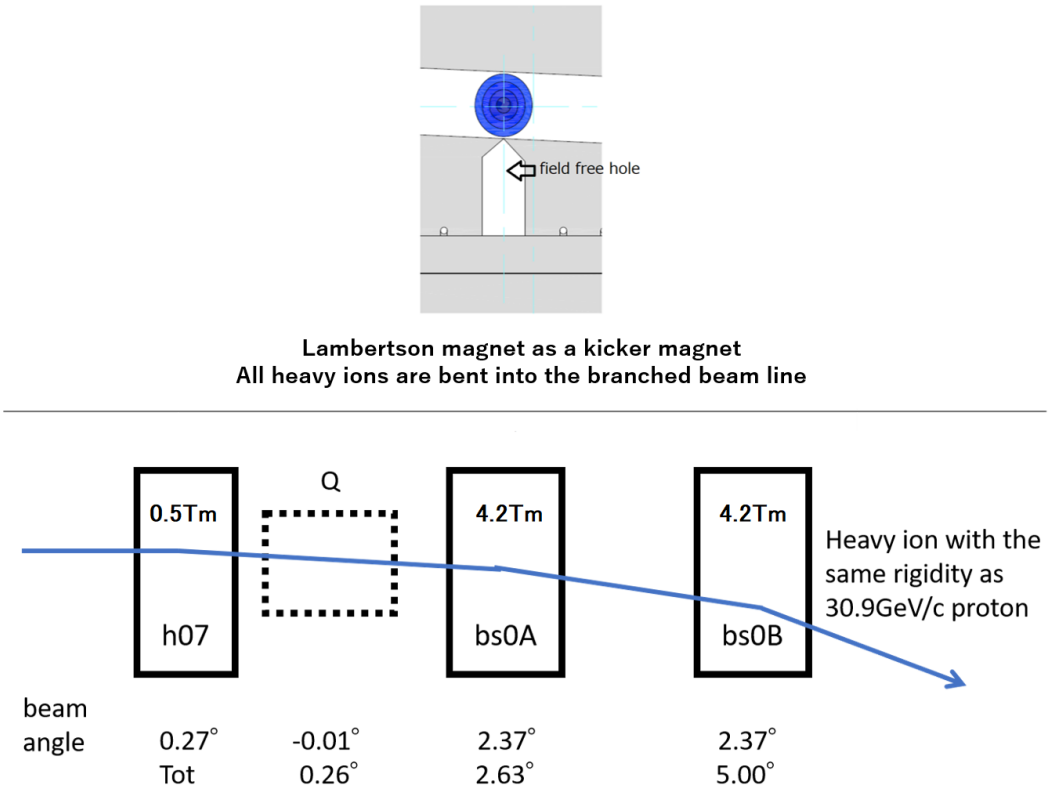

Figure 8: A conceptual view of the two two options at the beam branching point in the case of the heavy-ion beam. Upper panels:the Lambertson magnet option. Lower panel:the beam swinger option.

magnet. Then, all part of the heavy-ion beam is bent to the high-momentum beam line similarly to the J-PARC COMET experiment. The lower panel shows the beam swinger options. The heavy-ion beam is bent to the high-momentum beam line using the two beam swinger magnets similarly to the J-PARC E50 experiment.

The maximum beam rate at the high-momentum beam line for 30 GeV proton is 10^{10} per spill. The designed beam intensity of 10-AGeV heavy-ion beams is limited to the equivalent beam power for the proton beam to have similar radiation levels. In that case, we can utilize the existing beam dump and radiation shields. To confirm that, we performed simulations for radiation dose using MARS simulation code. We confirmed that with 1.2×10^8/spill 10 AGeV/c U beam, the radiation dose level at the accessible area around the experimental area is similar to that for 10^{10}/spill 30 GeV protons [32] within the limit of 25 μSv/h.

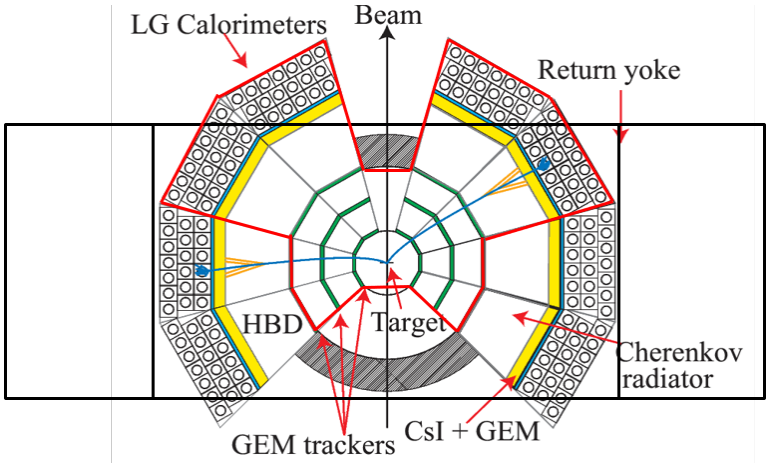

Figure 9: The top view of the E16 spectrometer for p+A collisions.

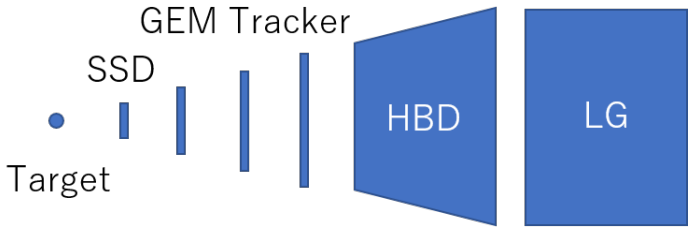

Figure 10: Schematic view of a module of the E16 spectrometer for p+A collisions.

2.3 The E16 Spectrometer

The layout of the E16 spectrometer is shown in Fig. 9 [33, 34]. The E16 is a fixed-target experiment with a large dipole magnet with the maximum vertical field of 1.8 T and BdL of $\sim$ 1.2 Tm from the target to the downstream.

The unit of the spectrometer is called a "module" which consists of a Silicon Strip Detector, three-planes of GEM trackers, and a Hadron-Blind Detector, and a Lead-Glass calorimeter from the target outward as shown in Fig. 10. One module covers the 30° horizontally and 30^o vertically. The charged particle track is reconstructed with SSDs and GTRs, and electron identification and pion rejection is done with HBDs and LGs. In Run 0 (2020-2021) and Run 1 (2022-) configurations, eight middle-layer modules (from $\sim \pm 30$ ∘) have been installed, while at Run 2, the full three-layer 26 modules are planned to be installed.

Silicon Strip Detectors (SSD) Silicon Strip Detectors (SSD) [35] is a inner-most tracking device which has excellent position resolution and operated at high rates. It is originally developed for the CBM experiment at FAIR. SSDs are located at $\sim$ 110 mm distance from the target. The sensor of the SSD is double-sided microstrip sensor. Its sensitive area is 60 mm (horizontal, x) $\times$ 60 mm (vertical, y). There are horizontal and stereo strips, which are placed in the different side. The strip pitch is 58μm and

we have the same pitch for the both sides.

GEM trackers (GTR) GEM tracker is a three-layer stack GEM detector operated with Ar-CO_2 mixture gas for charged particle track reconstruction [36]. The signals are detected in the horizontal (x) and the vertical (y) readout strips with the 0.35 mm width and 0.125 width, and 1.4 mm pitch and 0.464 mm effective width, respectively. The maximum particle rate for operation is expected to be $\sim$ 20 kHz/mm^2. The effective area of the three planes are 100 mm (x) $\times$ 100 mm (y), 200 mm $\times$ 200 mm, and 300 mm $\times$ 300 mm at the distance from the target of $\sim$ 220 mm, $\sim$ 430 mm, and $\sim$ 610 mm, respectively.

Hadron Blind Detectors (HBD) Hadron Blind Detector is a window-less and mirror-less Cherenkov detector in a proximity focus configuration. CF_4 gas behaves both as a Cherenkov radiator and chamber gas for the GEM stack. A Cherenkov photon is converted into electrons by CsI photocathode evaporated on the top GEM surface, amplified with three-layer GEM stack, and detected finally with the readout pads at the bottom of the GEM stack. The hadron rejection power is about 10^2 while keeping the electron detection efficiency of 90 %.

Lead-glass calorimeter (LG) Lead-glass modules originally from TOPAZ experiment are used. The energy resolution is about 10 % for 1 GeV electron. The pion rejection power with HBD and LG of 10^{-3} in the trigger level and 10^{-4} in offline analysis is expected.

2.4 The E16 Spectrometer Upgrade

The present proposal is based on the current E16 spectrometer with the following upgrades for heavy-ion collision experiments.

1. Zero-degree calorimeter for centrality determination
2. Upgrade of detectors in the forward region
3. Upgrade of frontend electronics and data acquisition system

Zero-degree calorimeter is required to determine the centrality of heavy-ion collisions. Due to much higher multiplicity per A+A collision compared to p+A collision, the occupancy of the detectors in the forward angle becomes severe and we may have to replace some of the GEM trackers to high-granularity detectors such as SSDs. Current data taking rate is limited up to 1 kHz. In order to inspect 50 kHz Au-Au collisions, the data acquisition system must be upgraded. One approach is to improve trigger rate by optimizing the APV25 readouts and upgrading FPGA firmware. Another approach is to utilize the triggerless and free streaming data taking system, which has been under development in ALICE [37] and LHCb [38] at the CERN-LHC.

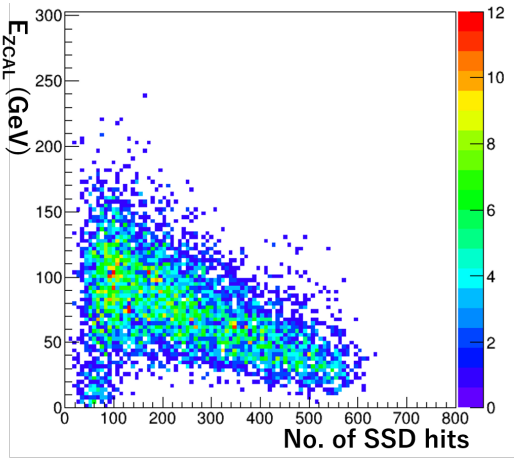

Figure 11: The energy deposit in ZCAL (GeV) vs the number of hits in SSDs.

2.4.1 Centrality Detectors

The centrality of heavy-ion collisions will be defined with the zero-degree calorimeter (ZCAL) and SSDs. ZCAL measures the energy of beam fragments, and SSDs measure the multiplicity of an event. The design of the calorimeter is based on RHIC zero-degree calorimeter [39]. The calorimeter is a sampling calorimeter consisting of 78 stacks of a 5-mm thick tungsten absorber plate and 1.4-mm space for PMMA scintillating fibers. The outer dimensions will be 150 mm (horizontal), 300 mm (vertical), and 500 mm (beam direction). The length in the beam direction corresponds to 4.0 λ_I and 11 X_0. The front face of ZCAL is located at 4.5 m downstream position from the target, which is just in front of the beam dump at 5 m. Fig. 11 shows the simulated correlation between the number of hits in SSD and the energy in ZCAL using JAM event generator and GEANT4, which indicates the anti-correlation. Using this correlation, we will select the centrality as the online trigger, and in the offline analysis.

2.4.2 Detector Upgrades in the Forward Region

Figure 12 shows a schematic view of the positions of 26 modules. Four modules around the beam will be upgraded.

Following upgrades will be applied in the 4 modules.

- The first layer of the GEM Tracker will be replaced by SSDs.
- Lead glass calorimeter will be replaced by a fine-segmented crystal $PbWO_4$ calorimeter.

The fine-segmented crystal $PbWO_4$ calorimeter has the same design as ALICE PHOS detector[40]. The crystal size of the PHOS detector is $2.2 \times 2.2 \times 18$ cm^3 and each crystal has an Avalanche Photo-diode readout. In the proposed experiment, one module contains 33 by 33 crystals.

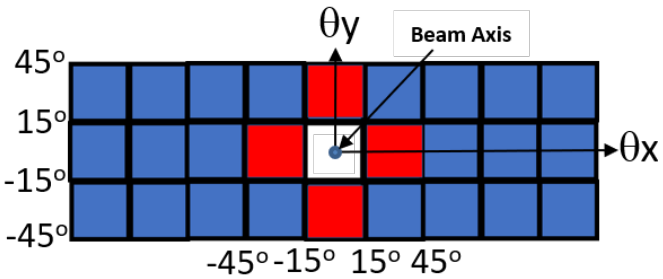

Figure 12: A schematic view of positions of 26 modules. The θ_x is defined as $\tan^{-1} x/z$, and θ_y is defined as $\tan^{-1]} y/z$. Modules shown in red will be upgraded.

2.4.3 Readout and DAQ Upgrade

We expect the beam intensity of 1.0×10^8 per 2 sec beam spill. With 0.1 % interaction length of the target thickness, the minimum bias event rate will be 100 k events/spill and 50 kHz. Current E16 data acquisition system is limited to 1 kHz [41, 42]. This limitation will be eliminated by decreasing the number of readout samples in APV25 chips used for GEM trackers and HBD, developing the FPGA firmware in the ADC board to allow to do online processing such as zero-suppression and feature extraction like clustering and standalone tracking, and sending compressed data from the ADC board to the computing servers or storage through 10GbE or InfiniBand network. These improvements will enable to run at 30 kHz trigger rate.

The field of nuclear experiments and high energy physics experiments is currently in a paradigm shift in a data acquisition system from the traditional triggered readout system to the free streaming readout system. The free streaming readout system eliminates the hardware trigger and utilizes the software-based online data processing and reconstruction and imposes the trigger decision in software. The ALICE [37] and LHCb [38] at the LHC will introduce the free streaming readout system in Run 3 and future CBM experiment at GSI-FAIR will also use the similar architecture in the data acquisition system. The front-end APV chips used in GEM trackers and HBD will be replaced by the one which supports the continuous readout such as SAMPA chip used in ALICE. Data from SAMPA chip will be sent to the computing nodes, where hardware acceleration devices such as FPGA and GPU are installed and used to perform online data processing such as feature extraction, event building, and full tracking and compress the data by the factor of $\sim 1/100$. These technologies are under development in ALICE, where it is aimed at processing 3 TB/s raw data and converting to the compressed data with 50 GB/s. Figure 13 shows the possible configuration of the logical data flow for the new DAQ upgrade, where the data chain from SSDs is not yet included. Raw data with the size of 2.3 TB/s is zero-suppressed on the SAMPA chips and is reduced up to 50 GB/s. Zero-suppressed data is further pushed to PCIe-based FPGA board such as ALICE-CRU [43], that is housed in the first level processing node (FPN). Data is further processed and clustering and tracklet calculations using three GEM layers will be performed to reduce the size up to 10 GB/s. Pre-processed data in

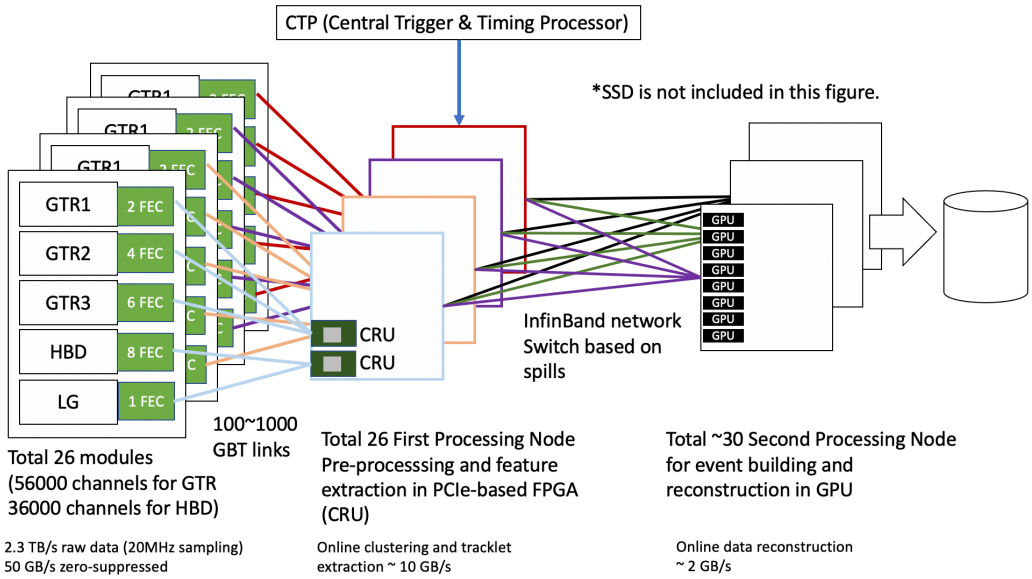

Figure 13: the hardware pipeline and the estimated throughput at different stages and and number of processing nodes

all FPNs is further pushed to the second level processor nodes (SPN). One SPN handles data from all FPNs in one spill (2 sec) and performs event building, full tracking, and electron identification. Finally, electron objects selected by loose cuts will be stored in the disk. A fraction of raw data will be also recorded in the storage.

2.5 Detector Occupancy and Efficiencies

Efficiencies assumed at the original E16 experiment Table 3 shows an electron identification efficiencies assumed at the original E16 experiment. These efficiencies are taken into account to evaluate the expected yield as described in Sec. 3.

Item	Efficiency	
Electron ID (HBD)	63%	For a single track
Electron ID (LG)	90%	For a single track

Table 3: Efficiencies for electron identification.

Efficiencies due to high hit multiplicities Even with the upgraded detectors, efficiency loss occurs due to a high hit multiplicity. Table 4 shows inefficiencies for the upgraded detectors. As a result, the total efficiency of 46% for a single track in the most central collisions should be taken into account to evaluate the final yield. Note: Only one of y positions measured in the 2nd and 3rd layers of the GEM tracker are required.

		Channel	Efficiency loss
SSD	X	1024	7.2%
	U	1024	7.2%
GTR 2nd layer	X	572	18%
	Y	144	32%
GTR 3rd layer	X	858	12%
	Y	216	20%
HBD		1400	3%
$PbWO_4$		1089	6%

Table 4: Efficiency losses of the upgraded detectors in central heavy-ion collisions..

3 Feasibility and Expected Results

3.1 Simulation Study

We performed simulation studies to evaluate physics performance for the di-electron measurements with the J-PARC E16 spectrometer. We used the nuclear cascade code JAM [44] to generate Au+Au at 10 AGeV/c collisions and used GEANT4 to account for the detector response and finite detector acceptance. The full 26 modules were assumed for the E16 spectrometer. The detector responses were implemented in the GEANT4 simulation based on the detector performances achieved in beam tests and earlier commissioning runs. The 35 μm-thick Au target was assumed, corresponding to 0.1% interaction probability in the case of an Au beam. For simplicity, we only considered π^0 decay, the γ conversion in the Au target, and mis-identified $\pi^{\pm}$ (99.9% rejection was assumed) as the background sources of di-electrons. Another note is that only electron and positron pairs were injected to the GEANT4 simulation and those detector responses, tracking, and PID performances under high multiplicity were not taken into account. The inefficiency of 46% for a single track under high multiplicity (Sec. 2.5) was taken account as a scaling factor to obtain the final signal yields.

To evaluate the cross section and obtain the kinematical distribution (y and p_T) of light mesons contributing to the di-electron measurement (π^0, η, ω, and ϕ), the JAM model was used as an event generator. Figure 14 shows the invariant yield distributions of the light mesons at mid-rapidity in central Au+Au collisions (0 $\leq$b$\leq$ 4 fm), where b is the impact parameter.

The fit functions of the previous experimental data at BNL-AGS given at Refs. [45, 46] are also shown in Fig. 14 for comparison. The solid line represents $(\pi^+ + \pi^-)/2$ in 0-5% Au+Au collisions at 8 AGeV/c [45] and the dashed line represents ϕ in 0-5% Au+Au collisions at 11.7 AGeV/c [45], respectively. In Fig. 14, the η distribution is scaled by 1/0.43, which is reported as the η/π^0 ratio in S+S collisions at 200 AGeV/c [47]. The ω/π^0 ratio at mid-rapidity in this JAM calculation is 0.113, while it is 0.096 at the CERES cocktail calculation [48]. The invariant m_T ($m_T \equiv \sqrt{p_T^2 + m_{meson}^2 - m_{\pi 0}^2}$) distributions of light mesons in the JAM are shown on almost the same curve with an appropriate scaling factor, where the nice agreement is visible.

In this proposal, two physics cases were considered for the thermal di-electron productions. One is the case when there is no phase transition and the temperature (T) is 150 MeV, which is based on the results of the coarse-graining transport approach in Fig. 4. The other is the case when there is a first-order phase transition and T is 120 MeV, which is based on the parameterization of a reduced critical temperature (T_c) at finite μ_B as $T_c(1-0.0066(\mu_B/T_c)^2)$ [49] and at $\mu_B = 500$ MeV and $T_c = 130$ MeV [18].

Figure 15 shows the yields of thermal low mass di-leptons ($0.3 < M_{l^+l^-} < 0.7$ GeV/c^2) normalized to the number of $\pi^{\pm}$ as a function of the collision energy from various experiments [14, 13, 50, 51, 52]. The normalized thermal di-lepton yield seems not to be very energy dependent. We assumed the normalized yield to be 1.2×10^{-5} (indicated as a red line in Fig. 15) in J-PARC-HI energy range. Since $dN_{\pi^{\pm}}/dy\ |_{y_{CM}=0}$ was 105 in the JAM model at central (0 <b< 4 fm) collisions, we assumed the thermal

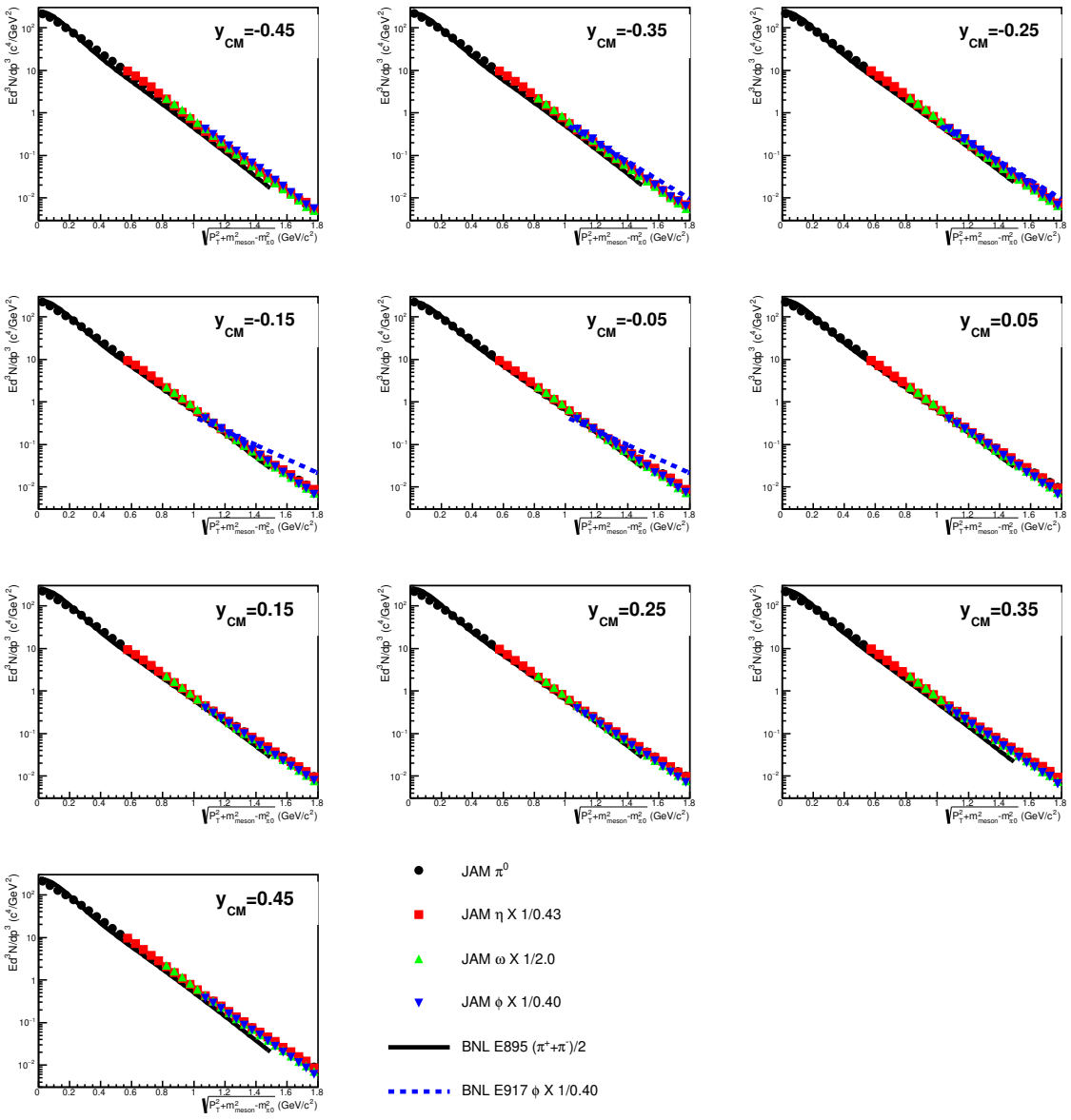

Figure 14: Invariant yield distributions of the light mesons (π^0, η, ω, and ϕ) generated by the JAM at mid-rapidity regions in central Au+Au collisions (0 <b< 4fm). The fit functions of the previous experimental data at BNL AGS given at Ref. [45, 46] are also indicated.

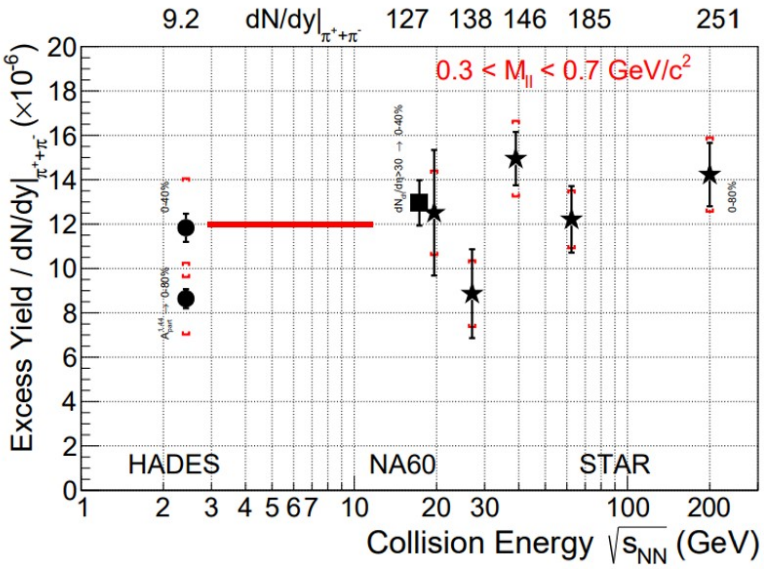

Figure 15: The yields of thermal low mass di-lepton ($0.3 < M_{l^+l^-} < 0.7$ GeV/c^2) normalized to the number of $\pi^{\pm}$ as a function of collision energy in previous experiments [14, 13, 50, 51, 52]. This Figure is taken from Ref. [53].

di-electron yield with $0.3 \leq M_{e^+e^-} \leq 0.7$ GeV/c^2 at the mid-rapidity ($\mid y_{CM} \mid \leq 0.5$) to be 1.26×10^{-3}, while in the case of minimum bias collisions ($0 \leq$ b ≤ 16 fm), $dN_{\pi^{\pm}}/dy \mid_{y_{CM}=0} = 100$ and $dN_{ee}/dy \mid_{y_{CM}=0} = 4.6 \times 10^{-4}$) in $0.3 \leq M \leq 0.7$ GeV/c^2. The invariant mass spectrum of the thermal di-electrons was assumed to be proportional to $(MT)^{3/2} \exp(-M/T)$ in all the mass ranges. The invariant p_T distribution and the rapidity distribution were assumed to be $\exp(-p_T/T)$ and flat, respectively. Figure 16 shows the reconstruction efficiency of the di-electron pairs with $T = 150$ MeV using the E16 spectrometer. In Fig. 16, the electron identification efficiency equivalent to the E16 experiment was assumed while the inefficiency due to high multiplicity was not taken account.

The E16 spectrometer has good acceptance for the di-electron pairs with high mass at mid-rapidity. In addition, low p_T pairs can be reconstructed. Therefore, it is possible to extract the temperature not only by the invariant mass spectrum but also by the p_T distribution as shown in Fig. 3.

The di-electron invariant mass spectra were evaluated for those two cases. Figure 17 shows the reconstructed invariant mass spectrum of electron pairs at mid-rapidity ($1 < y_{lab} < 2$) in the case of 100-day run with T=150 MeV and T=120 MeV. A combinatorial background is the dominant source of the backgrounds above 0.1 GeV/c^2. S/B depends on mass range but is in the order of 1/100. A precise evaluation of the combinatorial background is necessary to extract the signal pairs. Such evaluations have already been made in several previous experiments. For example, the PHENIX experiment reported about 0.2% uncertainty for the combinatorial background subtraction in central Au+Au collisions [54]. Since this uncertainty is determined by the

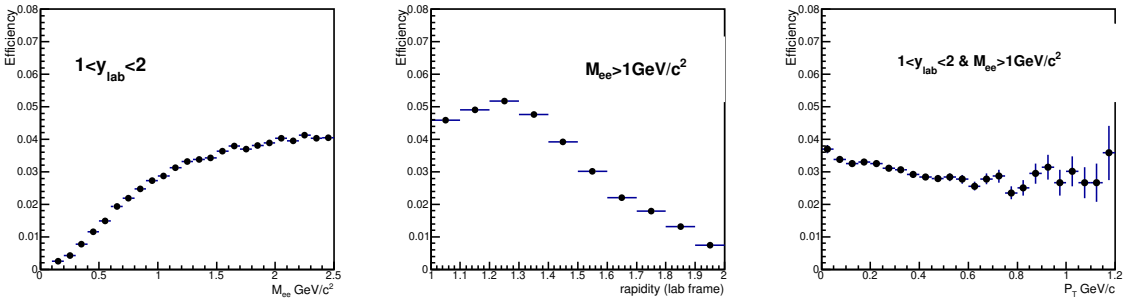

Figure 16: The reconstruction efficiency of di-electron pairs with $T = 150$ MeV using the J-PARC E16 spectrometer. The electron identification efficiency equivalent to the E16 experiment was assumed, while the inefficiency due to high multiplicity was not taken account.

statistics, it can be expected that the uncertainty of combinatorial backgrounds in J-PARC Au+Au collisions will be similar to the 0.1% level. When the 0.1% uncertainty is assumed for the combinatorial backgrounds, 1-10% of the uncertainties are assigned in the subtraction of backgrounds since background uncertainty is propagated through $(S/B)^{-1}$ to the uncertainty of signals. Roughly speaking, the systematic error is dominant over the statistical error below 0.6 GeV/c^2 (10% level or more) and the statistical error is dominant above 0.6 GeV/c^2 except for ω, ϕ resonance region. Figure 18 shows the reconstructed invariant mass spectrum after the combinatorial background subtraction at mid-rapidity ($1 \leq y_{lab} \leq 2$) in central collisions with 100-day run. ω and ϕ mesons are clearly observed and $\sim$ 30000 ω and $\sim$ 8000 ϕ can be collected with $S/N > 20$ only in central collisions. The p_T and y dependence of $\Gamma(\phi \to e^+e^-)/\Gamma(\phi \to K^+K^-)$ is expected to be studied precisely. The temperature extraction can be determined with an accuracy of about 10% by using only $M > 1.1$ GeV/c^2 with 100-day run in the case of 150 MeV. On the other hand, in the case of 120 MeV, it is difficult to determine precisely the temperature using only $M > 1.1$ GeV/c^2. However, it can be expected to achieve an accuracy of about 10% if $M \geq 0.7$ GeV/c^2 is used, although an additional careful treatment is necessary.

3.2 Beam Time Request

We request 100 days for the beam time with the 12 AGeV Au beam at the intensity of 1.0×10^8 ions per spill to complete the first measurement. It is highly preferred that the measurement is performed in a single beam year, but it is also possible to split the measurement over a few years. A systematical study for the beam energy at J-PARC is also important to discover the first-order phase transition, although measurements at other facilities will play a complementary role. This time, we will submit the proposal for the first measurement at the energy, which is considered to be the most important. For the beam energy scan, we will make another proposal.

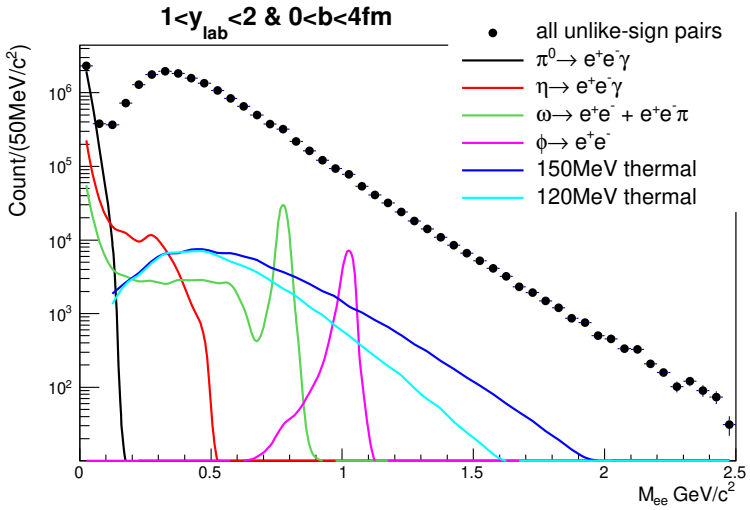

Figure 17: The reconstructed invariant mass spectrum of electron pairs in the case of 100-day run. Acceptance is not corrected.

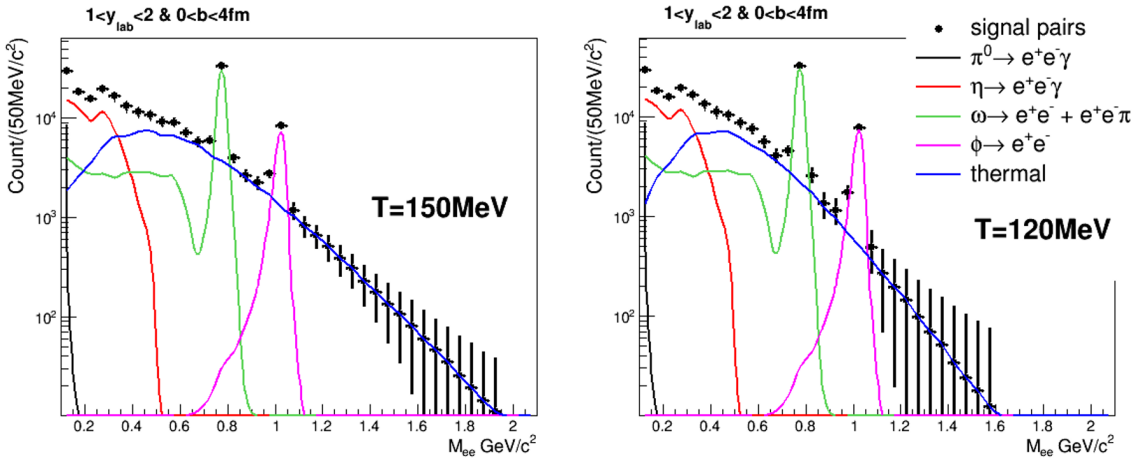

Figure 18: The reconstructed invariant mass spectrum after the combinatorial background subtraction at mid-rapidity ($1 \leq y_{lab} \leq 2$) in central collisions with 100-day run. Statistical error is only plotted, and acceptance is not corrected. Right panel: T=150 MeV. Left panel: T=120 MeV.

4 Schedule and Cost

The schedule of the experiment depends on the construction schedule of heavy-ion accelerators at J-PARC. The construction period of the heavy-ion injector including the connection to RCS will be around 5 years since the budget has been approved. We assume that 26 modules of E16 spectrometer are complete at so called E16 Run 2 beam time, which is expected 2023 or later. From these considerations in the experiment side, the earliest start time of the experiment may be 2026 or later. The start time of the experiment will be after the project of the extension of the Hadron Experimental Facility is approved.

The costs for the upgrade of the spectrometer are shown in Table 5. The costs include the replacement of the forward trackers and electromagnetic calorimeters, the construction of the zero-degree calorimeter, and the upgrade of part of front-end electronics and the new data acquisition system.

System	Amount	Unit price (k-Yen)	Cost (k-Yen)
SSD			
Sensor	16	400	6400
FEE	16	750	12000
Control modules	2	3000	6000
Other Equipment	1	10000	10000
$PbWO_4$ detectors			
Crystals	4400	27	118800
PIN-preamp unit	4400	15	66000
FEE	4400	5.5	24200
Other equipment	1	30000	30000
Zero-degree calorimeter			
Tangsten Plates	78	500	39000
Scintillating fiber sheet	78	50	3900
PMT	78	100	7800
DAQ			
Upgrades of data transfer	10	2000	20000
Total			344100

Table 5: Costs for the detector upgrade.

A Long Term Plans for J-PARC-HI project

This proposal is the first heavy-ion collision experiment at J-PARC utilizing the upgraded E16 spectrometer. The aim of this experiment is at elucidating a new state of matter composed of quarks and gluons and a first-order deconfiment or chiral phase transition by measuring di-electron invariant mass and momentum spectra at various mass ranges, collision spices, and collision centralities.

Our final experimental goals beyond this proposal are to explore the QCD phase structures such as the critical point, phase boundary of the deconfinement and chiral phase transitions, quarkyonic matter and color superconductivity, and to characterize the properties of new states of matter at the densities as high as 5 - 10 times the normal nuclear density using the world's highest beam rate of 10^{11} Hz [55].

We will propose and perform a series of heavy-ion experiments in the future, with either dedicated setups for some specific measurements or a general purpose detector setup for covering as much observable as possible. We will describe briefly the future perspectives for QCD matter physics and strangeness physics, which will be largely expended using high intensity heavy ion beams at J-PARC.

A.1 Accelerators, Facility, and Spectrometer

For the heavy-ion acceleration of the designed full beam intensity of 10^{11} Hz, we will build a new booster synchrotron and a 20 AMeV linac as shown in Fig. 19. The design of the high-intensity heavy-ion injector and the design parameters are summarized in Subsection 2.1.

Here we briefly explain a few specific features of the heavy-ion acceleration scheme to achieve high-intensity beam acceleration. A new charge-exchange injection scheme from the linac to the booster ring is adopted, and ions with multiple-charge states can be accelerated in the booster ring . In this scheme, with many injection turns, very high-intensity beams can be accumulated. For the injection from the booster ring to RCS, high-charge state beam (U^{86+} for U) is used so that RCS has minimum beam loss with its vacuum level of 10^{-6} Pa.

Experiments with full-intensity 10^{11} heavy-ion beams require strong radiation shields and beam dump, compared to those in the E16 experimental area. Also a large acceptance spectrometer is designed to perform various physics measurements proposed below, which requires large area. We are considering to extend the current high-momentum beam line and construct a new large acceptance spectrometer in the annex building outside the extended Hadron Experimental Facility, as shown in Fig. 20.

The conceptual design of the large acceptance J-PARC-HI spectrometer is shown in Fig. 21. Inside the large superconducting dipole magnet, a Time Projection Chamber (TPC) is positioned as a central tracking detector. The forward angles are covered with Silicon Pixel Trackers (SPTs), for its good rate capability. Time-of-Flight counters and Hadronic Calorimeter identify charged particles and electron/photons respectively. The centrality is defined with Zero-degree Calorimeter and the multiplicity measured in SPTs. The spectrometer is used for various measurements for hadrons, and their correlations and fluctuations. For the dilepton measurements other particle identifi-

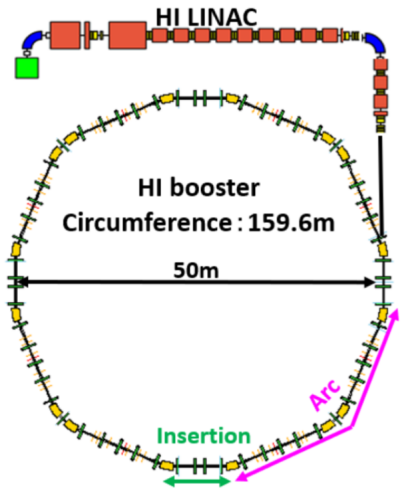

Figure 19: The new booster synchrotron and HI linac for the full HI beam intensity.

cation devices such as a ring-imaging charenkov counter, and muon trackers will be introduced.

Another smaller dipole magnet in front of the larger one is used for the closed geometry experiment to measure beam spectator particles, by sweeping out and stopping low momentum particles in the collimator inside the front magnet, and only high-momentum particles/nuclei with a specific rigidity is transported to the TPC and then decays of those particles/nuclei are reconstructed and identified. We will search for various hypernuclei and exotic particles such as strangelets and strange dibaryons.

It will take around five years to construct the full intensity HI injector. The schedule for the construction of the annex building and the large acceptance spectrometer will be after the building construction of the extended Hadron Experimental Facility is completed.

A.2 QCD Matter Physics

Our future heavy-ion experiments will supply invaluable experimental information on the following subjects.

A.2.1 QCD Phase Structure

It has been theoretically predicted that the QCD phase diagram in the temperature (T)–baryon chemical potential (μ_B) plane has a first-order phase boundary and a critical point, although the locations and properties of those have not yet been determined. Therefore, one of the major goals of the future experiments is to determine these phase structures experimentally by utilizing high-intensity heavy-ion beams.

Fluctuation observables are important probes that can retain information on the degree of freedom of the partonic phase. In particular, the collision energy dependence of the event-by-event fluctuations of various conserved charges may be promising observ-

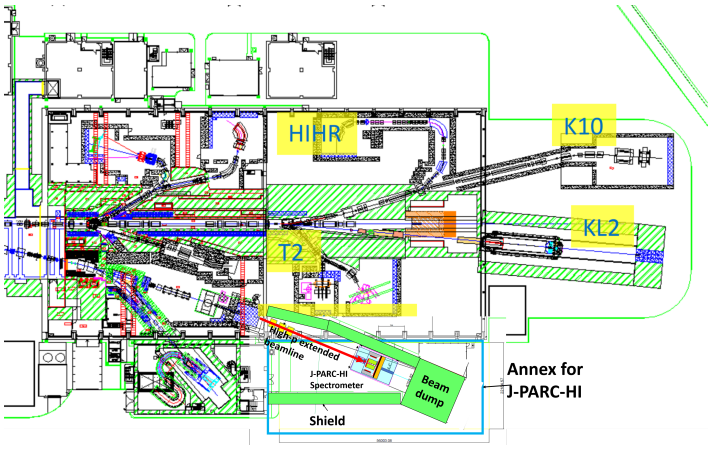

Figure 20: A future view of the extended high-momentum beam line for heavy-ion transportation and an annex for J-PARC-HI spectrometer with the extended Hadron Experimental Facility.

ables in the search for the QCD critical point and the onset of the deconfinement phase transition [56]. Recently, non-Gaussian fluctuations of conserved charges characterized by higher-order cumulants have been of particular interest [57].

Experimentally, the event-by-event analysis of fluctuation observables requires significant statistics, especially for higher-order cumulants. In this respect, JPARC-HI is highly suitable for performing the event-by-event analysis of non-Gaussian fluctuations and cumulants. Current heavy-ion experiments do not measure neutrons but instead evaluate the cumulants of the proton number as a proxy of the baryon number, resulting in large uncertainties. The event-by-event measurement of neutrons together with protons enables direct analysis of baryon number cumulants. At J-PARC-HI, neutron fluctuations will be measured for the first time.

It is expected that the matter at high density and at low temperature undergoes a phase transition from hadronic matter to a color superconductivity, which is believed to exist in the neutron stars [58]. The quark matter in a color superconducting phase is characterized by the formation of a di-quark condensate. One possible experimental approach to study the di-quark structure at high baryon density is enhanced di-lepton pair productions by the decays of gluons to di-electrons as a consequence of mixture of a photon and a gluon in the color superconductivity and by the pair-annihilations of the di-quark soft modes developed near the phase boundary. Another promising probe for studying the color superconductivity is to measure the charmed baryons such as Λ_c. The charm quarks are impurity of the medium. If charm quarks are embedded into the liquid state of $[ud]$ di-quarks, the production of Λ_c is enhanced since the direct two-body coalescence process between c quark and $[ud]$ di-quark is in favor compared to the normal three-body coalescence process between c, u, and d quarks. The enhancement of Λ_c production in ultra-high energy heavy-ion collisions at RHIC and LHC has been under discussion [59] experimentally and theoretically, where di-quark correlation is expected to exist near the critical temperature in strongly coupled

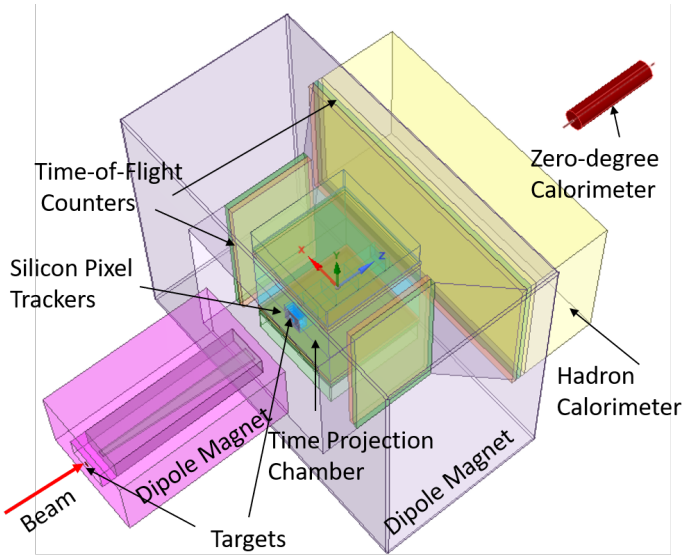

Figure 21: A conceptual design of the large acceptance heavy-ion spectrometer.

Quark-Gluon Plasma observed at RHIC and LHC energies.

At the J-PARC energies, production of charm quark pairs is just above the production energy thresholds and cross-section is expected to be very small. However, in nuclear collisions at the J-PARC energy, the secondary baryon interactions for particle production lowers the thresholds and consequently, we will be able to measure Λ_c with substantial statistics owing to high rate beams at J-PARC [60].

A.2.2 Characterizing the Properties of the New State of Matter

Heavy-ion collisions at intermediate energy (3-20 GeV) will also become a unique experimental tool for creating and studying dense media with baryon densities at 5 - 10 times larger than the normal nuclear density, that is comparable to conditions at the cores of neutron stars. The onsets of exotic phases, such as hyperons, strange quark matter, color superconductivity, are expected to occur in this region. Understanding the properties of dense media, especially the EoS and transport properties, is important to understand the internal structure of compact stars. One example of the measurements to explore the properties of dense matter is collective flow in heavy-ion collisions. The collective flow carries a wide range of information on the dynamical evolution of the hot medium created by heavy-ion collisions. In particular, the collective flow is tightly related to the EoS in the early stage because the pressure gradient of the medium is one of the sources of the flow. Precise measurements of the flow would therefore provide us with insights into the EoS of the hot and dense medium.

Another example is to use heavy quarks to explore the transport properties of the new matter. Heavy quarks are impurities of the medium composed of light quarks. In such this case, a scattering between a heavy quark and a light quark near and Fermi surface, which is mediates by gluon-exchange interactions, is enhanced as it is known

as the QCD Kondo effect [61]. This results in the fact that the electric resistivity is enhanced and the shear viscosity is suppressed. One of the success at RHIC and LHC is to characterize the transport properties using heavy quarks. From the energy loss and collective flow of low p_T heavy quarks, one can extract the diffusion constant. Similarly, the measurements of momentum and flow of heavy quarks at J-PARC will elucidate the transport properties of the matter at high baryon density.

A.3 Strangeness Nuclear Physics

Proposed energetic heavy ion beams at J-PARC will also be powerful tools for studying strangeness nuclei, so called hypernuclei that are sub-atomic systems with bound hyperon(s). The feasibility of the production and observation of hypernuclei as projectile fragments produced by induced reaction of heavy ion beams at a fixed target was already demonstrated by the HypHI collaboration at GSI employing the ^{6}Li+^{12}C reaction at 2 A GeV [62]. Since the velocity of the produced hypernuclei as projectile spectators by this reaction is similar to that of the projectiles, the lifetime of the produced hypernuclei becomes longer by its Lorentz factor, for example, approximately three for the beam energy of 2 A GeV. At the energy of heavy ion beams with J-PARC HI, the Lorentz factor will be > 10 for $N = Z$ projectiles, the mean decay length of the produced hypernuclei can be long enough that the produced hypernuclei can be separated and selected in-flight from other nuclear fragments by a strong magnetic field inside a compact super-conducting dipole magnet. The selected hypernuclear candidates of interest will be reconstructed behind the magnet via an invariant mass method by measuring four-momentum of all charged particles produced by the hypernuclear decays. It will provide an opportunity to search for very rarely produced exotic hypernuclei such as negatively-charged hypernuclei with Ξ^- hyperon. Furthermore, direct measurements of magnetic monets of hypernuclei can be measured by using the same experimental system. Lambda hyperons can be spin-aligned after the production of heavy ion beams, therefore, produced hypernuclei can be spin-aligned if the spin-alignments of the Λ-hyperon and the projectile spectator are coherently coupled. A precession of the spin-aligned hypernuclear state will take place inside of the magnetic field which is used for separating and selecting hypernuclear candidates [63]. With an assumption that the hypernuclear magnetic moment is equal to that of the free-Λ-hyperon, a precession angle of 68 degrees is expected in a magnetic field with a magnetic rigidity of 6 Tm. This large precession angle will enable a precise direct measurement of hypernuclear magnetic moments without any assumption in the hypernuclear structures, and it will give us insight of modifications of baryon properties contributed at quark-levels in nuclear mediums.

References

[1] L. Adamczyk et al. ΛΛ Correlation Function in Au+Au collisions at $\sqrt{s_{NN}} = 200$ GeV. Phys. Rev. Lett., 114(2):022301, 2015.

[2] Akira Ohnishi, Kenji Morita, Kenta Miyahara, and Tetsuo Hyodo. Hadron–hadron correlation and interaction from heavy–ion collisions. Nucl. Phys. A, 954:294–307, 2016.

[3] Shreyasi Acharya et al. First Observation of an Attractive Interaction between a Proton and a Cascade Baryon. Phys. Rev. Lett., 123(11):112002, 2019.

[4] M. Asakawa and K. Yazaki. Chiral Restoration at Finite Density and Temperature. Nucl. Phys. A, 504:668–684, 1989.

[5] Akira Ohnishi. Approaches to QCD phase diagram; effective models, strong-coupling lattice QCD, and compact stars. J. Phys. Conf. Ser., 668(1):012004, 2016.

[6] Nguyen Van Hieu and Pham Xuan-Yem. Gluon-photon mixing in dense qcd. Phys. Rev. D, 64:074009, Sep 2001.

[7] Teiji Kunihiro, Masakiyo Kitazawa, and Yukio Nemoto. How do diquark fluctuations and chiral soft modes affect di-lepton production in the deconfined phase? PoS, CPOD07:041, 2007.

[8] J. Pochodzalla *et al.* Probing the Nuclear Liquid-Gas Phase Transition. Phys. Rev. Lett, 75:1040, 2000.

[9] Ralf Rapp. Theory of Soft Electromagnetic Emission in Heavy-ion Collisions. Acta Phys. Pol. B, 42:2823, 2011.

[10] T. Galatyuk *et al.* Thermal dileptons from coarse-grained transport as fireball probes at SIS energies. Eur. Phys. J. A, 52:131, 2016.

[11] R. Arnaldi et al. NA60 results on thermal dimuons. Eur. Phys. J. C, 61:711–720, 2009.

[12] R. Arnaldi et al. Evidence for radial flow of thermal dileptons in high-energy nuclear collisions. Phys. Rev. Lett., 100:022302, Jan 2008.

[13] H. J. Specht *et al.* Thermal dileptons from hot and dense strongly interacting matter. AIP Conf. Proc, 1322:1, 2010.

[14] J. Adamczewski-Musch *et al.* Probing dense baryon-rich matter with virtual photons. Nature Phys, 15:1040, 2019.

[15] A. Senger and P. Senger. Probing Dense QCD Matter: Muon Measurements with the CBM Experiment at FAIR. Particles, 4:205, 2021.

[16] R.-A. Tripolt. Electromagnetic and weak probes: Theory. Nucl. Phys. A, 1005:121755, 2021.

[17] R. Rapp and H. van Hees. Thermal dileptons as fireball thermometer and chronometer. Phys. Lett. B, 753:586, 2016.

[18] H. T. Ding *et al.* Chiral Phase Transition Temperature in (2+1)-Flavor QCD. Phys. Rev. Lett, 123:062002, 2019.

[19] Tetsuo Hatsuda and Su Houng Lee. Qcd sum rules for vector mesons in the nuclear medium. Phys. Rev. C, 46:R34–R38, Jul 1992.

[20] S. Damjanovic. Thermal dileptons at SPS energies. J. Phys. G, 35:104036, 2008.

[21] Florian Seck, Tetyana Galatyuk, Ayon Mukherjee, Ralf Rapp, Jan Steinheimer, and Joachim Stroth. Dilepton Signature of a First-Order Phase Transition. 10 2020.

[22] Prashanth Jaikumar, Ralf Rapp, and Ismail Zahed. Photon and dilepton emission rates from high density quark matter. Phys. Rev. C, 65:055205, 2002.

[23] M. Kitazawa, T. Koide, T. Kunihiro, and Y. Nemoto. Precursor of color superconductivity in hot quark matter. Phys. Rev. D, 65:091504, 2002.

[24] Chi Yang. The star beam energy scan phase ii physics and upgrades. Nucl. Phys. A, 967:800, 2017.

[25] Andras Laszlo. The na61/shine experiment at the cern sps. Nucl. Phys. A, 830(1):559, 2009.

[26] J. Friese. HADES, the new electron-pair spectrometer at GSI. Nucl. Phys. A, 654(1):1017c, 1999.

[27] M. .B. Golubeva *et al.* Nuclear-nuclear collision centrality determination by the spectators calorimeter for the MPD setup at the NICA facility. Physics of Atomic Nuclei, 76:1, 2013.

[28] T. Ablyazimov *et al.* Challenges in QCD matter physics –The scientific programme of the Compressed Baryonic Matter experiment at FAIR. Eur. Phys. J. A, 53:60, 2017.

[29] Tetyana Galatyuk. Future facilities for high μ_B physics. Nucl. Phys. A, 982:163–169, 2019.

[30] Hiroyuki Harada *et al.* Simulation Study of Heavy Ion Acceleration in J-PARC. JPS Conf. Proc., 33:011028, 2021.

[31] T. Iwashita *et al.* KEK digital accelerator. Phys. Rev. ST Accel. Beams, 14:071301, 2011.

[32] H. Sako and K. Aoki. Preliminary Study of Radiation from Heavy-Ion Beams at J-PARC Hadron Experimental Facility. Proc. of 16th Annual Meeting of Particle Accelerator Society of Japan, pages 344–347, 2019.

[33] S. Yokkaichi et al. Proposal Electron pair spectrometer at the J-PARC 50-GeV PS to explore the chiral symmetry in QCD. the 1st PAC meeting, Fri 30 June - Sun 02 July, 2006.

[34] S. Yokkaichi et al. J-PARC E16 Run0 Proposal. the 24th PAC meeting, Mon 24 - Wed 26 July, 2017.

[35] M. Deveaux and J. M. Heuser. The silicon detector systems of the Compressed Baryonic Matter experiment. PoS, Vertex2013:009, 2013.

[36] Yusuke Komatsu, Kazuya Aoki, Yoki Aramaki, Hideto En'yo, Koki Kanno, Daisuke Kawama, Shinichi Masumoto, Wataru Nakai, Yuki Obara, Kyoichiro Ozawa, Michiko Sekimoto, Takuya Shibukawa, Tomonori Takahashi, Yosuke Watanabe, and Satoshi Yokkaichi. Development of the gem tracker for the j-parc e16 experiment. Nucl. Instrum. Method. A, 732:241–244, 2013. Vienna Conference on Instrumentation 2013.

[37] P. Buncic, M. Krzewicki, and P. Vande Vyvre. Technical Design Report for the Upgrade of the Online-Offline Computing System. 4 2015.

[38] Guoming Liu and Niko Neufeld. DAQ Architecture for the LHCb Upgrade. J. Phys. Conf. Ser., 513:012027, 2014.

[39] C Adler, A Denisov, E Garcia, M Murray, H Stroebele, and S White. The rhic zero degree calorimeters. Nuclear Instruments and Methods in Physics Research Section A: Accelerators, Spectrometers, Detectors and Associated Equipment, 470(3):488–499, 2001.

[40] D. C. Zhou. PHOS, the ALICE-PHOton Spectrometer. J. Phys. G, 34:S719–S723, 2007.

[41] T. N. Takahashi et al. Data acquisition system in Run-0a for the J-PARC E16 experiment. In 22nd IEEE Real Time Conference, 10 2020.

[42] T. N. Takahashi et al. The electronics, online trigger system and data acquisition system of the J-PARC E16 experiment. J. Phys. Conf. Ser., 664(8):082053, 2015.

[43] Upgrade of the ALICE Readout & Trigger System. 2013.

[44] Y. Nara *et al.* Relativistic nuclear collisions at 10 AGeV energies from p+Be to Au+Au with the hadronic cascade model. Phys. Rev. C, 61:024901, 2000.

[45] J. L. Klay *et al.* Charged Pion Production in 2 to 8 AGeV Central Au+Au Collisions. Phys. Rev. C, 68:054905, 2003.

[46] B. B. Back *et al.* Production of ϕ mesons in Au+Au collisions at 11.7 AGeV/c. Phys. Rev. C, 69:054901, 2004.

[47] R. Albrecht *et al.* Production of η Mesons in 200 AGeV S+S and S+Au Reactions. Phys. Lett. B, 361:14, 1995.

[48] G. Agakichiev *et al.* Systematic study of low-mass electron pair production in p-Be and p-Au collisions at 450 GeV/c. Eur. Phys. J. C, 4:231, 1998.

[49] O. Kaczmarek *et al.* Phase boundary for the chiral transition in (2+1)-flavor QCD at small values of the chemical potential. Phys. Rev. D, 83:014504, 2011.

[50] L. Adamczyk *et al.* Bulk properties of the medium produced in relativistic heavy-ion collisions from the beam energy scan program. Phys. Rev. C, 96:044904, 2004.

[51] L. Adamczyk *et al.* Energy dependence of acceptance-corrected dielectron excess mass spectrum at mid-rapidity in collisions at $\sqrt{s_{NN}}$= 19.6 and 200 GeV. Phys. Lett. B, 750:64, 2015.

[52] J. Adam *et al.* Measurements of Dielectron Production in Au+Au Collisions at $\sqrt{s_{NN}}$= 27, 39, and 62.4 GeV from the STAR Experiment. arXiv:1810.10159[nucl-ex].

[53] T. Galatyuk. Recent Results from HADES. JPS Conf. Proc, 32:010079, 2016.

[54] A. Adare *et al.* Detailed measurement of the e^+e^- pair continuum in p+p and Au+Au collisions at $\sqrt{s_{NN}}$= 200 GeV and implications for direct photon production. Phys. Rev. C, 81:034911, 2010.

[55] H. Sako et al. Letter of Intent for J-PARC Heavy-Ion Program. the 22nd PAC meeting, Wed 27 - Fri 29 July, 2016.

[56] Volker Koch. Hadronic Fluctuations and Correlations. 2010.

[57] Masayuki Asakawa and Masakiyo Kitazawa. Fluctuations of conserved charges in relativistic heavy ion collisions: An introduction. Prog. Part. Nucl. Phys., 90:299–342, 2016.

[58] Mark G. Alford, Andreas Schmitt, Krishna Rajagopal, and Thomas Schäfer. Color superconductivity in dense quark matter. Rev. Mod. Phys., 80:1455–1515, 2008.

[59] Su Houng Lee, Kazuaki Ohnishi, Shigehiro Yasui, In-Kwon Yoo, and Che-Ming Ko. Lambda(c) enhancement from strongly coupled quark-gluon plasma. Phys. Rev. Lett., 100:222301, 2008.

[60] J. Steinheimer, A. Botvina, and M. Bleicher. Sub-threshold charm production in nuclear collisions. Phys. Rev. C, 95:014911, Jan 2017.

[61] Shigehiro Yasui and Sho Ozaki. Transport coefficients from the qcd kondo effect. Phys. Rev. D, 96:114027, Dec 2017.

[62] C. Rappold et al. Hypernuclear spectroscopy of products from ^{6}Li projectiles on a carbon target at 2A GeV. Nuclear Physics A, 913:170 – 184, 2013.

[63] T. R. Saito et al. Hypernuclei with Stable Heavy Ion Beam and RI-beam Induced Reactions at GSI (HypHI). Letter of Intent submitted to GSI G-PAC, 2005.